Mechanism design for coordinating vehicle-based mobile sensing tasks within the ride-hailing platform

Shenglin Liu[1], Qian Ge*[1], Ke Han†[2], Daisuke Fukuda[3], and Takao Dantsuji[4]

[1]*School of Transportation and Logistics, Southwest Jiaotong University, Chengdu, China*
[2]*School of Economics and Management, Southwest Jiaotong University, Chengdu, China*
[3]*Department of Civil Engineering, The University of Tokyo, Tokyo, Japan*
[4]*Institute of Transport Studies, Monash University, Australia*

Abstract

This paper evaluates the benefit of integrating vehicle-based mobile crowd-sensing tasks into the ride-hailing system through the collaboration between the data user and the ride-hailing platform. In such a system, the ride-hailing platform commissions high-valued sensing tasks to idle drivers who can undertake either ride-hailing or sensing requests. Considering the different service requirements and time windows between sensing and ride-hailing requests, we design a staggered operation strategy for ride-hailing order matching and the sensing task assignment. The auction-based mechanisms are employed to minimize costs while incentivizing driver participation in mobile sensing. To address the budget deficit problem of the primal VCG (Vickrey-Clarke-Groves)-based task assignment mechanism, we refine the driver selection approach and tailor the payment rule by imposing additional budget constraints. We demonstrate the benefits of our proposed mechanism through a series of numerical experiments using the NYC Taxi data. Experimental results reveal the potential of the mechanism for achieving high completion rates of sensing tasks at low social costs without degrading ride-hailing services. Furthermore, drivers who participate in both mobile sensing tasks and ride-hailing requests may gain higher income, but this advantage may diminish with an increasing number of such drivers and higher demand for ride-hailing services.

Keywords: Mechanism design, mobile crowd-sensing, ride-hailing system

1 Introduction

In the past decade, the ride-hailing industry emerged as a significant door-to-door transportation mode, reshaping urban mobility in many countries. However, the market's rapid growth appears to have slowed in its two largest markets, i.e., the United States (Statista, 2023) and China (Hanzhi, 2024), leading the ride-hailing platforms into fierce competition with both external and internal companies. This motivates ride-hailing platforms to explore new niche markets, including other vehicle-based crowd-sourced activities, alongside human mobility (Li et al., 2014). For example, food or freight delivery service constitutes a non-negligible part of the revenue of Uber (Uber-UK, 2023). In China, the problem is more subtle with the advent of third-party integrators of the ride-hailing service, such as Amap and Baidu. Many car rental companies enter the ride-hailing business by leasing vehicles to drivers and assigning the ride-hailing orders to them with the help of the integrators. In other words, the ride-hailing market itself is ironically a new niche market for car rental companies. Instead, some researchers and practitioners have explored the integration of taxi or ride-hailing service with vehicle-based mobile sensing (Xu et al., 2019; Wu et al., 2020).

*Corresponding author. Email: geqian@swjtu.edu.cn
†Corresponding author. Email: kehan@swjtu.edu.cn

In the mobile sensing system, either human workers or vehicles equipped with *ad hoc* sensors visit specified points of interest passively or in response to platform requests. They transmit collected data to processing systems and receive rewards from data users. This sensing approach has been applied to a variety of scenarios in urban management, including pollution monitoring (Hasenfratz et al., 2015; Jezdovi et al., 2021), infrastructure maintenance (Eriksson et al., 2008), and traffic congestion management (Guo et al., 2022). However, vehicle-based mobile sensing is limited by sampling bias due to the sensitivity of the resulting dataset to the vehicles' mobility patterns. Although dedicated sensing vehicles offer high levels of sensing flexibility and reliability since they are *fully controllable* to fulfill very specific sensing requirements (Ji et al., 2023), the costs associated with their procurement, operation, and maintenance make large-scale deployment in the road network challenging for data users. Consequently, there is a need for data users to identify cost-effective alternatives for collecting sensing data, thereby reducing expenditure on dedicated sensing vehicles.

Inspired by this, we investigate an operational strategy for vehicle-based mobile crowd-sensing that integrates sensing tasks with ride-hailing requests, incentivizing drivers to undertake tasks while maintaining service levels for regular riders. In this business model, a data user collaborates with a ride-hailing platform by releasing a third-party app for sensing tasks and commissioning these tasks to a pool of available drivers. These drivers are *semi-controllable* because they are autonomous in selecting the tasks but their service patterns could be altered by the data users or platform by incentivization. Both the driver and the ride-hailing platform receive commissions from the data user for successfully completed sensing tasks. Any remaining sensing tasks, such as areas where no driver is available, would be handled by a dedicated vehicle fleet owned by the data user. This approach allows the data user to cut down its own vehicle fleet for data sensing, enables drivers to earn extra income through side gigs, and may increase revenue for the ride-hailing platform. The operational strategy is illustrated in Figure 1.

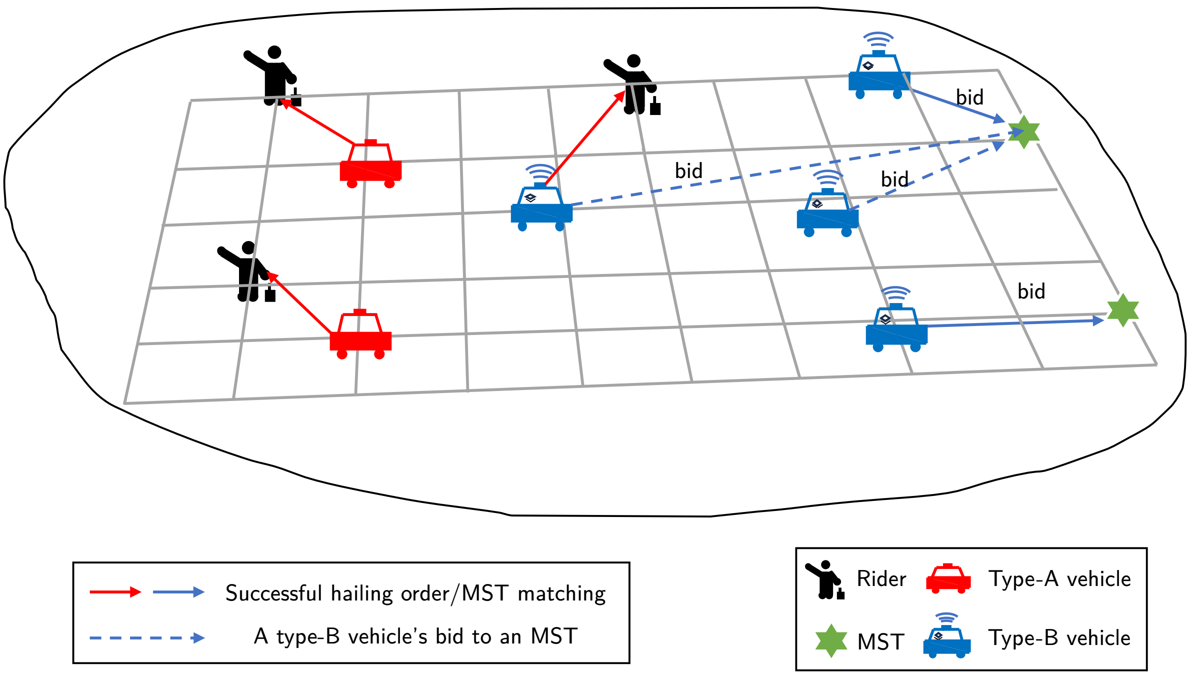

Figure 1: Schematic of the ride-hailing order and MST assignment system. Type-A vehicles are exclusively designated for ride-hailing orders, whereas Type-B vehicles have the flexibility to handle both passenger delivery and mobile sensing tasks. Initially, the ride-hailing platform matches vehicles with riders and then allocates mobile sensing tasks to the remaining Type-B vehicles through an auction-based procedure.

For the data user, a sensing point of interest (PoI) constitutes an individual sensing task, navigating a vehicle with sensing device to this location for a brief stop to collect data. It usually takes the driver several minutes to obtain a complete data sample. Hence, sensing tasks could be outsourced to ride-hailing platforms by generating an equivalent number of 'artificial ride-hailing requests' at PoIs and assigning these tasks to drivers through the similar procedure used for ordinary trip requests. While this strategy may benefit the data user, it may not align with the operational objectives of the ride-hailing platform, which must prioritize trip requests to ensure service levels and maintain customer loyalty. Additionally, sensing tasks differ from trip requests not only in their spatial distributions and pickup/drop-off time windows (or earliest commencement and latest completion times for sensing tasks), but also in factors such as quantity, service quality and driver commitment. The regular driver-rider matching pattern, along with the prescribed taxi fare for ordinary ride-hailing requests, may not be suitable for sensing tasks. More crucially, the completion rate of sensing tasks might not attain an ideal objective without the active involvement of drivers, and it would be imprudent to mandate the acceptance of drivers concerning these tasks. For the ride-hailing platform, the process of trip matching should not be hindered or negatively influenced by the introduction of a series of sensing tasks. To tackle these challenges, the ride-hailing platform may need to implement different rules for matching drivers with mobile sensing tasks (MSTs) and ride-hailing requests.

To the best of our knowledge, this paper presents the first operational strategy for addressing the integrated mobile sensing and ride-hailing task assignment problem within a unified ride-hailing system, aimed at benefiting all involved stakeholders. Specifically, our objectives are as follows:

(i) How can we ensure that all stakeholders, including the data user, the ride-hailing platform, and the drivers, derive benefits or, at the very least, do not suffer any negative impact from the introduction of MSTs to the ride-hailing platform?

(ii) What methods can be employed to incentivize drivers to accept and successfully complete sensing tasks?

(iii) How to conduct sensing tasks while maintaining a satisfactory service level of trip matching?

(iv) Given a limited budget from the data user, how can we achieve adequate coverage of areas of interest through vehicle-based mobile crowd-sensing?

(v) What is the impact of system design parameters on the effectiveness of the operational strategy?

We make the following contributions in this paper:

(i) We introduce an operational strategy for the ride-hailing platform that coordinates the assignment of trip requests and mobile sensing tasks. Previous studies have highlighted that while dedicated vehicles for sensing tasks offer strong reliability and flexibility, their high costs make large-scale deployment within road networks challenging (Han et al., 2024). The strategy proposed in this paper provides the data user with the potential to reduce sensing costs, including the expenses associated with procurement, operation, and maintenance of dedicated vehicles, as well as the costs of recruiting and training full-time drivers.

(ii) While formalizing trip request matching as a bipartite graph matching problem, we commission mobile-sensing tasks to drivers through an auction-based approach. This approach is a refinement of the classical Vickrey-Clarke-Groves (VCG) mechanism, with an added guarantee on the total budget. This refinement ensures favorable economic properties such as individual rationality (IR), incentive compatibility (IC), and budget balance (BB).

(iii) We evaluate the performance of the proposed model framework on the TLC Trip Record Data. Computational results demonstrate that our coordinated operational strategy offers the benefits of the data user, ride-hailing platform, and drivers without compromising service levels for ride users. Furthermore, our refined mechanism reduces the total cost of mobile sensing compared to the VCG mechanism.

The remainder of this paper is organized as follows. Section 2 reviews literature related to this study. Section 3 presents the model framework for coordinating the trip matching and the task assignment problems. Our refined mechanism for task assignment and its economic properties are described in Section 4. Section 5 summarizes the main results and the managerial insights of computational experiments. Section 6 concludes this work.

2 Literature review

This paper explores the coordination strategy of trip matching and task assignment within the ride-hailing platform. We categorize the related literature into three main streams: (1) vehicle-based mobile crowdsensing, with an emphasis on the use of taxis, (2) coordination of ride-hailing services with delivery or other tasks, and (3) auction-based mechanisms for resource allocation in transportation.

2.1 Taxi-based mobile crowdsensing

Vehicles are widely used for mobile crowdsourced tasks, especially urban data collection, and crowdsourced delivery, for their advantages in high mobility, scattered distribution, and low cost. The mobile crowdsensing tasks could be performed either by *active data collectors* who are primarily dedicated to the sensing tasks or *passive data collectors* who record the data while conducting other tasks. There are large studies addressing the data collection, completion, assimilation, and training problems of active data collectors for mobile sensing. One may refer to (Ji et al., 2023) for a recent review on this topic.

Our work focuses exclusively on ride-hailing taxis, which fall in the group of passive data collectors. In contrast to the active data collectors, the routes and trajectories of the taxis could not be planned or coordinated by a centralized operator, i.e., the sensing power is sensitive to the driving and cruising behavior of taxi drivers(O'Keeffe et al., 2019). Some unpopular streets or areas are rarely or even never visited by taxis. Nonetheless, providing information on the spatial and temporal demand to the drivers will affect their behaviors and welfare increase among drivers (Zhang et al., 2020). Further explorations on the mobility behavior of taxi drivers may refer to Wang et al. (2019).

Instead of controlling the trajectories of taxis directly, for which the effect is doubted, a more realizable solution is to develop incentive mechanisms to motivate the drivers to cover the ideal areas (Ji et al., 2023). Masutani (2015) develop a routing control scheme that recommends routes to a subset of vehicles that maximize the sensing quality. Fan et al. (2019) applies the reverse combinatorial auction to motivate taxi drivers to perform the sensing tasks following the scheduled trajectories. Xu et al. (2019) and Chen et al. (2020) navigate the idle taxis mounted with sensors to achieve desirable sensing quality. A comparable incentive mechanism is proposed to motivate drivers to follow the navigation. Asprone et al. (2021) calculates a set of ε-minimum routes for partial vehicles such that sensing coverage is maximized, in which the cost of any ε-minimum route is less than that of the minimum cost route multiplied by a predefined parameter ε.

The existing studies assume that a taxi can only be dedicated to either conducting sensing tasks or serving passengers. However, this assumption does not accurately conform to reality and tends to overestimate the success rate of drivers in undertaking sensing tasks. It overlooks the opportunity costs involved in conducting regular work, which could affect drivers' willingness to undertake sensing tasks. This observation motivates us to develop an operational strategy that integrates sensing tasks, though small in quantity compared to ride-hailing orders, into the regular workflow of drivers. In this approach, we assume the drivers are rational and choose sensing tasks based on their net utility. To our knowledge, this approach is novel in the literature on taxi-based mobile sensing.

2.2 Coordination of multiple tasks in the taxi network

The literature on the coordination of multiple heterogeneous crowd-sourcing tasks within the taxi/ride-hailing network is new and fast-growing (Alnaggar et al., 2021). An promising attempt is the Share-a-ride problem (SARP) in which a mixed integer linear program is formulated to plan the set of sharing routes for passengers and parcels using the same fleet of taxis (Li et al., 2014; Ji et al., 2024). It is noted that people and freight delivery differ in many aspects such as price and service level. Nevertheless, the passengers should be prioritized in the person-freight shared taxi network. Chen et al. (2017) propose a heuristic strategy for collecting e-commerce reverse flow using taxis. For the sake of reducing environmental impact and promoting the revenue of drivers, only taxis with passengers on board are allowed to collect returned goods. The freight delivery with the mixed fleet of regular and occasional vehicles is studied as the Vehicle Routing Problem with Occasional Drivers (VRPOD) by Archetti et al. (2016). In such a problem, the number of regular drivers is unlimited but they may request high cost. Vice versa for the occasional drivers. Extensions to online and bundle delivery problems are made by Archetti et al. (2021) and Mancini and Gansterer (2022), respectively. There is also a vast of studies using the auction-based approach to commission delivery tasks to shippers (Zou and Kafle (2023) for example), their technical details will be reviewed in the next section. Despite its limitation in scalability (Qi et al., 2018), the potential economic benefit and operational flexibilities of the crowdsourced delivery make it particularly attractive to shippers. However, crowdsourced parcel delivery services differ from sensing tasks in terms of spatial distribution, request volume, and vehicle requirements. While parcel delivery strategies may offer some inspiration, further adaptation is needed for our study.

In addition to the integrated operation strategies for multiple crowd-sourcing tasks in the taxi network, one may also be curious about the business modes of their alliance. Unfortunately, no study is available on how heterogeneous tasks are coordinated by the same operator. However, a similar business mode in which different ride-hailing platforms for the same tasks are coordinated within one integrator has been studied by a handful of researchers. Zhou et al. (2022) first investigate the third-party platform integration in ride-sourcing markets and assumes the integrator could directly control the vehicle-ride request matching process, despite which ride-hailing platform a vehicle is affiliated to. Thus, the integrator is responsible for maximizing the number of realized hailing orders and social welfare respecting the equilibrium among ride-hailing platforms. Li et al. (2024) observe that the ride-hailing platforms may create a so-called 'artificial scarcity' market phenomenon by sacrificing the order completion rate for high profit, which is caused by the inappropriate pricing strategy of the integrator. They propose a Stackelberg game model for pricing to remove artificial scarcity. Bao et al. (2023) address a ride-hailing order assignment approach for the third-party integrator aiming at minimizing the waiting time of passengers.

Despite the abundance of literature on the market environment, business operation, and stakeholders' decision-making problems of the ride-hailing platform (Wang and Yang, 2019), there is limited study on the coordination of taxis for heterogeneous tasks by one operator. Before stepping into the technical details, the ride-hailing platforms are curious about problems such as whether will they benefit from the crowd-sourced tasks, how the crowd-sourced tasks are released dynamically, how the crowd-sourced tasks and ride-hailing requests are organized to guarantee the service level for passengers, how the targeted drivers are selected, how to commission the tasks to the appropriate drivers to avoid reluctance, etc. Our work will answer this operational problem when coordinating the sensing tasks and ride-hailing requests in the same taxi network.

2.3 Auction-based task allocation in mobility

Auction-based mechanism designs have been extensively used in various mobility task allocation problems such as shared rides matching (Yan et al., 2021; Bian et al., 2020), parcel delivery (Li et al., 2022) and mobile sensing task commission (Fan et al., 2019). The main motivation for using an auction-based assignment approach is to ensure the welfare of all stakeholders involved in the trading process. The auction approaches could be broadly classified into: (i) combinatorial auction, in which a bidder is allowed to submit price for multiple tasks in each round of auction (Hammami et al., 2021); (ii) sequential auction, in which the targets are released dynamically over time and are auctioned sequentially (Mochon et al., 2022; Kong et al., 2023); and (iii) double auction, in which both the supply and demand sides are allowed to make offers and the auction is settled by the auctioneer (Xu et al., 2017; Li et al., 2020). There are also research works that fall into the intersection of two groups, (Karamanis et al., 2020) for example, in using the combinatorial double auction for solving the ride-sharing assignment and pricing problems.

While numerous studies address task allocation issues in mobility services, the auctioning of mobile sensing tasks to ride-hailing drivers remains largely unexplored. The distinctive characteristics of these tasks, such as their sparse spatial distribution, flexible time requirements, and limited data volume, necessitate tailored approaches when implementing auctions. Moreover, concerns regarding budget deficits from both data users and ride-hailing platform operators in adopting taxi-based mobile sensing should also be addressed. Otherwise, data users may opt to utilize their dedicated vehicles for data collection. To tackle these challenges, we propose a novel auction-based mechanism for assigning mobile sensing tasks that excludes non-economical matching combinations and refines the payment rule.

3 Coordination of ride-hailing and mobile sensing tasks

This section delves into the coordination of ride-hailing requests and mobile sensing tasks within a single ride-hailing taxi fleet. The platform operates with two types of taxis: Type-A vehicles exclusively handle trip requests, while Type-B vehicles are equipped with sensing devices and can accommodate both trip requests and mobile sensing tasks. Denoting the sets of Type-A and Type-B vehicles as $\overline{\mathcal{D}}$ and $\widetilde{\mathcal{D}}$ respectively, it's worth noting that the fleet size of Type-B vehicles is typically smaller due to the higher costs associated with purchasing and installing sensing devices. The union of these sets, $\mathcal{D} = \overline{\mathcal{D}} \cup \widetilde{\mathcal{D}}$ represents the entirety of taxis registered with the ride-hailing platform.

Consider a study area comprising various locations identified for monitoring purposes, each corresponding to a pending sensing task. Given that the completion rate of sensing tasks hinges on the availability of active Type-B drivers, employing an auction-based task assignment method becomes favorable to motivate Type-B drivers to undertake sensing tasks. This incentivization is driven by the potential for Type-B drivers to earn a higher expected reward from sensing tasks compared to trip requests. To distinguish the difference of execution between passenger requests and sensing tasks, we segment the service time of Type-B vehicles, denoted as $\mathcal{T}$, into multiple decision-making cycles.

Figure 2 presents different phases of one complete decision-making cycle. Each complete decision-making cycle $T \in \mathcal{T}$ comprises three phases: (i) the exclusive trip matching phase (T_1), during which trip requests are assigned to both Type-A and Type-B vehicles; (ii) the trip matching and mobile sensing task bidding phase (T_2), in which Type-B drivers can bid on multiple sensing tasks while Type-A drivers continue to match trip requests; and (iii) the trip matching and mobile sensing task assignment phase (T_3), where sensing tasks are first allocated to Type-B vehicles through the rule of winner determination, followed by the

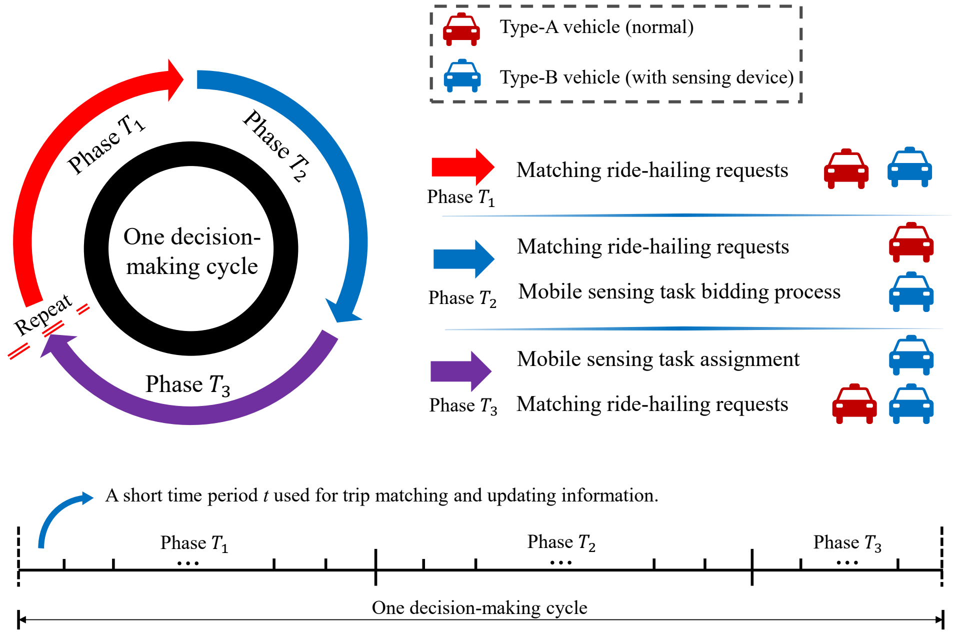

Figure 2: Phases of one decision-making cycle. A decision-making cycle is divided into three phases, which may be further subdivided into multiple time periods. In each time period t, a trip matching is performed once, and dynamic information regarding trip requests and sensing tasks is updated accordingly.

Table 1: Key parameters and variables

Indices and sets	
$\mathcal{D}_t$	Set of available drivers in the t-th interval (including both the Type-A and Type-B drivers)
$\widetilde{\mathcal{D}}_t$	Set of available Type-B drivers in the t-th interval ($\widetilde{\mathcal{D}}_t \subseteq \mathcal{D}_t$)
$\mathcal{R}_t$	Set of available riders in the t-th interval
$\mathcal{K}_t$	Set of task requests released in the t-th interval
A	Set of region in geographic network
Parameters and constants	
p_r^s	Base price charged from a matched rider r
L_0^s	Travel distance covered by the initial fare
t_0^s	Travel time covered by the initial fare
l_0	Average service distance of all trip requests
β_1	Incremental cost per unit travel distance when the distance exceeds L_0^s
β_2	Incremental cost per unit time when the time exceeds t_0^s
p_r	Total fare charged from a matched rider r
p_{dr}	Driver d's earning to pick up the rider r from the ride-hailing platform
$\overline{V}$	Average vehicle speed
f_m	Upper bound of opportunity cost in cruising time
ξ	Constant time cost in executing sensing task
L_{ub}	Maximum pick-up distance
α	Driver's expected earning per unit travel distance
$\overline{b}$	The upper bound of bid value
$\underline{b}$	The lower bound of bid value
μ	Coefficient for calculating opportunity cost in the task assignment
c_q	Operating cost per unit travel distance when using the dedicated vehicle
C	Base reward for a task request
Ω	Overall budget for sensing tasks
Decision variables	
x_{dr}^t	Binary variable equals to 1 if driver $d \in \mathcal{D}_t$ is matched with a rider $r \in \mathcal{R}_t$ are matched in the t-th interval, and 0 otherwise
x_{dk}^t	Binary variable equals to 1 if driver $d \in \widetilde{\mathcal{D}}_t$ is matched with a sensing task $k \in \mathcal{K}_t$ in t-th interval, and 0 otherwise

assignment of trip requests to Type-A drivers and any Type-B drivers who fail in sensing task assignment.

In the phase T_1, both Type-A and Type-B vehicles enjoy equal priority, and the operation of Type-A vehicles remains unaffected by the sensing task assignment in T_2 and T_3. By the end of phase T_1, the ride-hailing platform first checks the availability of Type-B vehicles and then determines whether to initiate an auction for sensing tasks and how many tasks to be assigned. If the number of idle Type-B drivers is below a specified threshold, no sensing tasks will be commissioned. In this case, the phases T_2 and T_3 will be dedicated to ride-hailing requests, similar to Phase T_1. The ride-hailing platform will evaluate whether to commission the sensing tasks in the next decision cycle.

In the phase T_2, the ride-hailing platform releases a specific number of sensing tasks. Each task forms an auction venue. Eligible drivers, including those Type-B drivers who shift to the idle state following the completion of a sensing task or trip request and those who fail to match any trip requests, are allowed to bid on multiple tasks. It should be noting that not all idle Type-B drivers will be selected by the ride-hailing platform for sensing tasks. Instead, a subset of the drivers is chosen such that they have limited impacts on rider service.

In the phase T_3, as the bidding concludes, the ride-hailing platform gathers bids from each auction venue. It then determines the winners and payoffs for each sensing task through a combinatorial auction process. Notably, the platform first assigns sensing tasks before conducting trip matching. Type-B drivers who submitted bids for sensing tasks but were not successfully assigned will join unmatched Type-A drivers in the trip-matching process. In other words, sensing tasks are assigned to a subset of Type-B drivers at the beginning of the phase T_3, while trip matching continues throughout this phase, involving both idle Type-A and Type-B drivers.

Some notations consistently utilized throughout this article are summarized in Table 1. The following assumptions are made for modeling the problem:

(1) The data user collaborates with the ride-hailing platform, providing a total budget for conducting sensing task assignment and then installing sensing devices onto Type-B vehicles. In addition, the ride-hailing platform releases a third-party app for assigning sensing tasks to a pool of available Type-B drivers.

(2) Drivers cannot simultaneously execute sensing tasks and ride-hailing requests.

(3) Each sensing task specifies a PoI. Upon arriving at the designated PoI, the driver performing the sensing task must make a brief stop to allow the sensing device to collect data at the location.

(4) A driver's private valuation for performing a sensing task is assumed to be a piecewise linear function dependent on distance.

3.1 Opportunity cost of drivers

Within the set of trip requests and MSTs, certain remote requests may exist, with their destinations located in suburban areas. Serving these requests would require drivers to leave high-demand areas. Typically, although drivers could immediately return to high-demand areas after servicing remote requests, they may still be reluctant to accept such requests. This is particularly true when dropping off passengers in suburban or rural areas, as searching for subsequent MSTs or trip requests in low-demand regions often requires more time. Hence, in addition to the direct rewards from sensing tasks and trip requests, drivers often factor in opportunity costs when deciding whether to undertake a trip request or MST. In this study, we adopt different criteria to the assessment of opportunity cost in accepting trip requests and mobile sensing tasks.

3.1.1 The estimation of opportunity cost from trip requests

Opportunity cost from trip requests can be roughly estimated by considering a driver's expected waiting time at the destination for a new request. The expected waiting time for the next trip request depends on both the supply and demand at the destination, encompassing the number of available vehicles and trip requests. It is worth noting that these values can be estimated from historical data or calculated on the fly.

Let n_{aT} denote the estimated number of trip requests in the region a during the decision-making cycle T, n_{aT}^{taxi} denotes the estimated number of available drivers in the same region within this cycle, and T_0 indicates the duration of each cycle. Thus, $\frac{n_{aT}}{n_{aT}^{taxi}}$ signifies the anticipated number of trip requests allocated to each driver if they head towards region a during the decision-making cycle T. The expression $\frac{n_{aT}}{T_0 n_{aT}^{taxi}}$ represents the average number of trip requests matched per driver per unit of time. Consequently, we let its inverse $\frac{T_0 n_{aT}^{taxi}}{n_{aT}} = \Delta t$ correspond to the duration between completing one trip request and being matched with the next trip request in the region a, effectively denoting the estimated cruising time in that region. In addition, Assuming that the cruising time of any driver follows a uniform distribution $U[0, \Delta t]$, the expected cruising time is given by $\frac{\Delta t}{2}$. However, if n_{aT} is exceedingly small, Δt can become extremely large. To avoid such a situation, we may impose an upper bound f_m on the opportunity cost. Therefore, a driver's opportunity cost for picking up a trip request with the destination r_{d} in the cycle T is calculated by:

$$f(r_{\mathrm{d}}) = \min\left\{ f_m, \quad \alpha \overline{V} \cdot \frac{T_0 n_{a_{r_{\mathrm{d}}}T}^{taxi}}{2 n_{a_{r_{\mathrm{d}}}T}} \right\}, \tag{3.1}$$

where α is a driver's basic reward per unit travel distance, $\overline{V}$ is the average vehicle speed, and $a_{r_{\mathrm{d}}}$ is the area where the destination r_{d} is located. The Equation (3.1) will be incorporated into the driver's earning to pick up riders, as shown in Equation (3.4).

3.1.2 The estimation of opportunity cost from mobile sensing tasks

The procedure for calculating the opportunity cost of accepting a sensing task is different from that of accepting a trip request. If a Type-B driver accepts a sensing task, this driver may lose the opportunity to pick up any riders in the neighboring area after completing the sensing task. We note that the MSTs usually occur in remote areas with low trip demand rate, and the Type-B drivers may have to experience long deadheading trips after serving these tasks. Thus, their opportunity cost should account for the extra costs from deadheading distance and time duration of the sensing task at the destination.

Then, we can simplify the determination of opportunity cost by assuming it relies on the distance between the driver's current location and the PoI associated with the MST, the estimated deadheading time, and sensing time at the PoI. In this study, if the distance a vehicle travels to the designated PoI for a sensing task is less than the average distance of trip requests l_0, the driver only needs to consider time cost incurred by searching for next request and executing sensing task. This is because, in practice, the majority of trip requests are not long-distance, and accepting such sensing task typically does not produce extra distance-based cost. The sensing task's opportunity cost $g(l)$ can be expressed as a non-decreasing function of this distance and is incorporated into the driver's private valuation, as shown in Equation (3.12).

$$g(l) = f_m + \xi + \max\{0, \quad \mu(l - l_0)\} \quad \mu > 0 \tag{3.2}$$

Here, for simplicity, we directly let f_m be the deadheading time cost at the PoI associated with the MST. ξ denotes a constant time cost when a driver executes a sensing task at the

PoI. l denotes the shortest distance traveling to the PoI marked on a sensing task, whereas l_0 indicates the average service distance of all trip requests.

3.2 Trip matching problem

Trip matching model is established for finding potential matches between available drivers and newly arrived or backlogged trip requests. This matching procedure is executed sequentially in small time intervals during the decision-making cycle, regardless of whether it occurs in phase T_1, phase T_2, or phase T_3.

When the rider r is matched by the ride-hailing platform, the fare charged to the rider comprises several components: the initial hailing fare, additional distance- and time-based fares. The total fare p_r can be expressed as:

$$p_r = p_r^s + \max\{0, \beta_1(L_r - L_0^s)\} + \max\{0, \beta_2(t_r - t_0^s)\}, \tag{3.3}$$

where p_r^s represents the basic price set by the ride-hailing platform. The second term accounts for any additional distance-based fare when the shortest distance L_r from origin to destination exceeds the basic distance L_0^s. The third term represents any additional time-based fare when the actual travel time t_r exceeds the basic time t_0^s. L_0^s and t_0^s denote the base distance and time covered by the basic taxi fare, respectively.

When a driver d accepts the trip request from the rider r, this driver can receive the earning to pick up the rider r from ride-hailing platform. We let the earning p_{dr} from serving the rider r consist of two components: a distance-based fare and an additional fare arising from the opportunity cost shown in Equation (3.1). Such additional fare encourages the driver to take remote trip requests, thereby increasing the number of successful matches and regulating the distribution of vehicles across different regions (You et al., 2023).

$$p_{dr} = \alpha L_r + f(r_{\mathrm{d}}) \tag{3.4}$$

Here, p_{dr} is the driver d's earning to pick up the rider r from ride-hailing platform. L_r represents the shortest distance from the origin r_{o} of rider r's request to its destination r_{d}. $f(r_d)$ denotes the additional payment arising from the opportunity cost when a driver drops off rider r at the destination r_{d}.

Following the idea of Agatz et al. (2011), our objective function is minimizing the total pickup distance while maximizing the number of matched driver-rider pairs. These objectives can also be regarded as maximizing the total pickup distance saving. Let L_{dr} represent the pickup distance in time period $t \in T$. The saved distance for a driver-rider pair is calculated as $\sigma_{dr}^t = \max_{r \in \mathcal{R}_t}\{L_{dr}\} - L_{dr}$. We formulate the trip-matching problem as follows:

$$\max \sum_{d \in \mathcal{D}_t} \sum_{r \in \mathcal{R}_t} \sigma_{dr}^t x_{dr}^t \tag{3.5}$$

$$\text{s.t.} \quad \sum_{d \in \mathcal{D}_t} x_{dr}^t \leq 1, \quad \forall r \in \mathcal{R}_t \tag{3.6}$$

$$\sum_{r \in \mathcal{R}_t} x_{dr}^t \leq 1, \quad \forall d \in \mathcal{D}_t \tag{3.7}$$

$$(p_r^t - p_{dr}^t) x_{dr}^t \geq 0, \quad \forall d \in \mathcal{D}_t, r \in \mathcal{R}_t \tag{3.8}$$

$$\sigma_{dr}^t = \max_{r \in \mathcal{R}_t}\{L_{dr}\} - L_{dr}, \quad \forall d \in \mathcal{D}_t, r \in \mathcal{R}_t \tag{3.9}$$

$$L_{dr} x_{dr}^t \leq L_{ub}, \quad \forall d \in \mathcal{D}_t, r \in \mathcal{R}_t \tag{3.10}$$

$$x_{dr}^t \in \{0, 1\}, \quad \forall d \in \mathcal{D}_t, r \in \mathcal{R}_t \tag{3.11}$$

Constraints (3.6) and (3.7) ensure that each driver and rider can be assigned only once. Constraint (3.8) excludes assignments resulting in negative revenues, while constraint (3.10) prevents assigning riders to drivers who are excessively far from them.

The trip-matching problem can be viewed as a bipartite graph-matching problem, noting Constraints (3.8)-(3.10) can be calculated beforehand. This problem can be efficiently solved using the Kuhn-Munkres (KM) algorithm, which finds the maximum weight perfect matching on the bipartite graph $G(\mathcal{N}_t, E_t)$ representing drivers, riders, and their potential matches. In this graph, the vertices $\mathcal{N}_t$ comprise the set of drivers $\mathcal{D}_t$ and riders $\mathcal{R}_t$, while the edges E_t represent potential matches between drivers and riders, with weights corresponding to the cost σ^t_{dr} calculated by Equation (3.9).

To calculate the optimal matching, we initially eliminate the infeasible edges. Each vertex is then assigned an initial label: for one group of vertices, the labels are set to their maximum potential weights among all possible matches, while for the other group, the labels are set to 0. These labels are iteratively updated to identify augmenting paths in the bipartite graph. The algorithm terminates when no new matches are available. The KM algorithm is outlined in detail in Algorithm 1.

Algorithm 1: Kuhn-Munkres Algorithm

Input: The set of drivers $\mathcal{D}_t$, the set of riders $\mathcal{R}_t$, weight matrix W
Output: Optimal perfect matching

Construct a square matrix W by adding virtual drivers and riders;
Initialize a match M and labels for the drivers l_x and the riders l_y ;
for $u \in \mathcal{D}_t$ **do**
    while True do
        Reset all vertices to unvisited state;
        Find the augment path $p(u)$ for u;
        if no augment path exists **then**
            break;
        for $v \in \mathcal{R}_t$ **do**
            if v not visited **and** $l_x[u] + l_y[v] == W[u, v]$ **then**
                Find a augment path $p(v)$ for v;
                if v is not matched **or** $p(v)$ exists **then**
                    Augment path $p(u) \leftarrow (u, v)$;
                    $M \leftarrow (u, v)$;
        Find the tuple (u, v) that u is visited but v is not;
        Update each visited vertex's label with minimum $\Delta = l_x[u] + l_y[v] - W[u, v]$;

3.3 The primal VCG-based MST assignment (VCG-MST) mechanism

In order to achieve efficient and fair allocation of MSTs, we briefly introduce the framework of auction-based mechanism, i.e., the VCG-MST. This mechanism entails the participation of both the drivers and the platform. As indicated in Figure 3, the platform releases MSTs at the beginning of phase T_2, and then each Type-B driver can submit his/her unit-distance commission to a subset of MSTs to the platform. The plaform calculates the true valuation by collecting bids from all bidders. Then, the platform will allocate released MSTs to a subset of bidders in the phase T_3 in the auction decision-making process. This procedure is coined *winner selection*. Finally, the platform calculates the payments to drivers based on the *payment determination* procedure following the VCG rule.

The primary motivation for the data user collaborating with the ride-hailing platform to utilize Type-B vehicles for MSTs lies in reducing their costs associated with purchasing and maintaining dedicated sensing vehicles. In addition, the overall budget for sensing tasks is

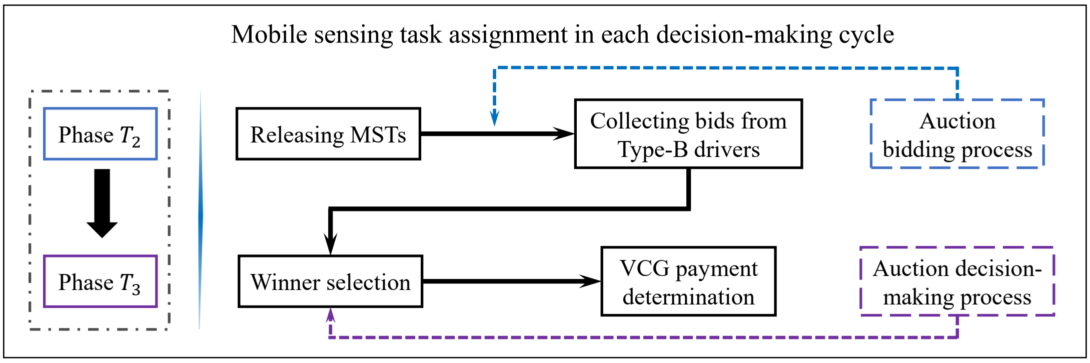

Figure 3: The framework of mobile sensing task assignment based on the VCG-MST mechanism.

provided by the data user, and the ride-hailing platform needs to regulate the expenditure of the budget. Hence, the objective of the MST assignment problem is to minimize expenses or maximize savings on expenses related to sensing tasks. Before constructing the MST assignment model, we firstly introduce the auction bidding process where Type-B drivers state their bidding information to the platform.

3.3.1 The auction bidding process

In the auction bidding process, the ride-hailing platform is responsible for the release of MSTs and the subsequent collection of bids from Type-B drivers. The bidding information is used for the purpose of informing the auction decision-making process and is provided by these participants. Therefore, it is a process that requires the participation of both parties. In this subsection, we intend to define a few terms for subsequent argumentation about bidding on the driver's side.

- *Private valuation.* The private valuation presents a Type-B driver's estimation of earning to an MST. It is a piecewise linear function, including the distance-based fare and opportunity cost of this driver.
- *Stated valuation.* The stated valuation refers to the price submitted by a Type-B driver to the platform through bidding. It comprises the base reward set by the platform for completing the sensing task and the driver's bid price.
- *True valuation.* The true valuation indicates the actual price that a Type-B driver would like to submit, defined as the maximum between the private valuation and the stated valuation. It will be collected by the platform for the purpose of informing the auction decision-making process.

In the t-th interval, the *private valuation* of Type-B driver d who would like to serve the sensing task k, denoted by $\underline{v}^t_{dk}$, is calculated based on distance-based fare and opportunity cost in Equation (3.2):

$$\underline{v}^t_{dk} = \alpha l_{dk} + g(l_{dk}) = \begin{cases} \alpha l_{dk} + f_m + \xi & l_{dk} \le l_0 \\ \alpha l_0 + (\alpha + \mu)(l_{dk} - l_0) + f_m + \xi & l_{dk} > l_0 \end{cases} \tag{3.12}$$

Here, the private valuation can be depicted as a piecewise linear function, and l_0 denotes the average service distance of all trip requests.

During the phase T_2 in each decision-making cycle, a Type-B driver $d \in \widetilde{\mathcal{D}}_t$ has the option to submit bids for a limited number of MSTs at the same unit price. In this study, drivers are permitted to freely determine the per-unit distance commission $\mathcal{B}_{dk}^t$ within a specified range through bidding. This value is incorporated into the driver's stated valuation and any valid bid $\mathcal{B}_{dk}^t$ must satisfy the following inequality:

$$\alpha \leq \underline{b} \leq \mathcal{B}_{dk}^t \leq \overline{b}. \tag{3.13}$$

Here, $\underline{b}$ and $\overline{b}$ denote the lower and upper bounds of the earning per unit distance, respectively. And α represents the expected earning per unit distance for serving a rider. Let c_q denote the sensing cost per unit distance of a dedicated sensing vehicle for completing a task. Furthermore, we assume $c_q \geq \overline{b}$. If driver d does not bid for an MST k, we set $\mathcal{B}_{dk}^t = +\infty$, preventing the pair (d, k) from being selected in the assignment model. It's important to note that all drivers independently submit their bids. In other words, any driver can not get access to bidding information from other drivers.

When a driver d is submitting a bid, a third-party app released by the platform automatically calculates the *stated valuation* based on the base reward, the bid and the shortest distance between this driver's location and PoI marked on the sensing task k. The driver d's stated valuation for MST k is calculated as follows:

$$\tilde{v}_{dk}^t = C + \mathcal{B}_{dk}^t l_{dk} \tag{3.14}$$

where C is the driver's base reward on completing an MST, and l_{dk} indicates the travel distance between driver d's current location and the location marked on sensing task k. It should be noting that when $l_{dk} = 0$, the driver d is located exactly at the PoI marked on the sensing task k. The base reward for sensing task should cover the opportunity cost incurred by deadheading time and sensing time as described in Equation (3.2). (e.g., $C \geq f_m + \xi$)

Intuitively, one might assume that the stated valuation would exceed the private valuation; however, this is not always the case. As we noted previously, a driver could submit his/her bid to the platform by simply inputting the unit-distance commission. The driver's valuation to an MST could be calculated based the unit-distance commission, the total distance of deadheading trip and the driver's opportunity cost. The platform could identify the *stated valuation* of a driver, as it is calculated by what the driver reports to the platform. However, this formula neglects the drivers increasing reluctance to overlong distance requests, which most likely take a form of piecewise linear function shown as the *private valuation*. Figure 4 illustrates the relationship between the stated valuation (3.14) and the private valuation (3.12) under different parameter settings. The figure on the right shows that the stated valuation is always above the private valuation. As for the figure on the left, we may calculate the intersection of two linear functions. Clearly, $l^* = \frac{C+\mu l_0 - f_m - \xi}{\alpha + \mu - \mathcal{B}_{dk}^t}$. When the distance $l_{dk} > l^*$, the stated valuation is less than the private valuation. In this case, the driver d may suffer a potential negative utility if this driver submit bidding information to platform according to the stated valuation.

For a rational driver, his or her utility, defined as the difference between the final earning and the private valuation, is not allowed to be negative. If the stated valuation is lower than the private valuation, submitting the stated valuation could result in a final earning, calculated by the mechanism, that falls below the private valuation. To prevent this issue, drivers could submit a formal request to the platform, allowing them to directly provide their private valuation to the system. The platform may raise the commission of an MST to the maximum of these two valuations to incentivize the driver to conduct sensing tasks. This maximum is named *true valuation*, defined as the maximum between the drivers stated valuation $\tilde{v}_{dk}^t$ and private valuation $\underline{v}_{dk}^t$, as shown in Equation (3.15):

$$v_{dk}^t = \max\left\{C + \mathcal{B}_{dk}^t l_{dk}, \alpha l_{dk} + g(l_{dk})\right\} \tag{3.15}$$

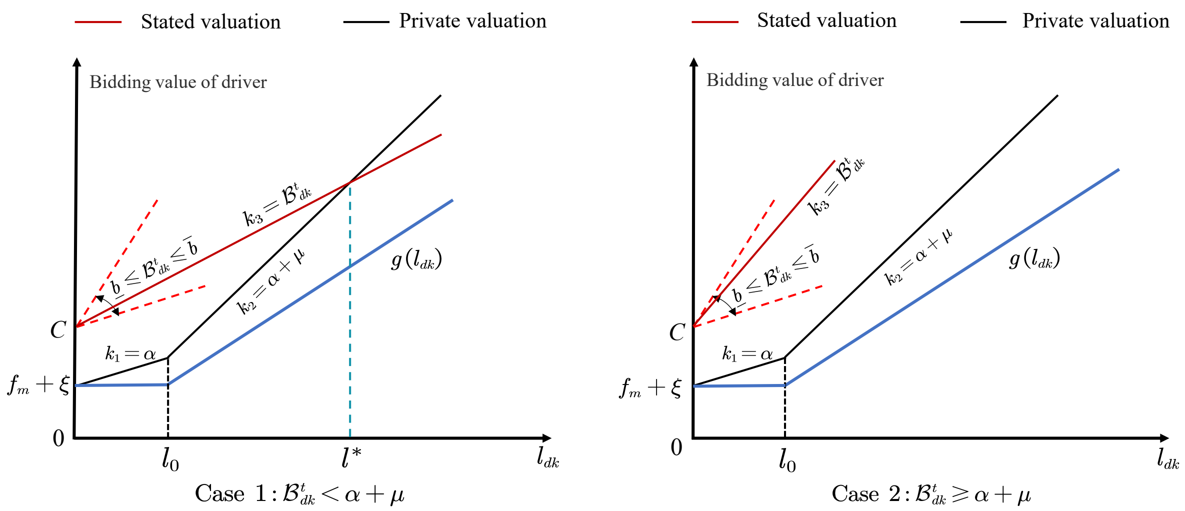

Figure 4: A driver's stated valuation and private valuation to a task. **Left**: When $\mathcal{B}^t_{dk} < \alpha + \mu$ and $l_{dk} \geq l^* = \frac{C+\mu l_0 - f_m - \xi}{\alpha+\mu-\mathcal{B}^t_{dk}}$, $\tilde{v}^t_{dk} < \underline{v}^t_{dk}$. This driver is allowed to submit the greater of two valuations as bidding information. **Right**: $\mathcal{B}^t_{dk} \geq \alpha + \mu$, $\tilde{v}^t_{dk} \geq \underline{v}^t_{dk}$. The stated valuation is always greater than the private valuation, and this driver can benefit from submitting stated valuation.

3.3.2 Winner selection

After the auction bidding process, the platform will collect true valuations for auction decision-making process.

In this study, the *sensing cost saving* δ^t_{dk} quantifies the cost reduction achieved by assigning the MST to a Type-B driver instead of dispatching a dedicated vehicle. This cost reduction is computed as follows:

$$\delta^t_{dk} = c_q \cdot l_{qk} - v^t_{dk}. \tag{3.16}$$

Here, c_q represents the unit cost per unit distance when using a dedicated vehicle, while l_{qk} denotes the distance from the nearest depot of dedicated vehicles to the MST k, which can be estimated by the shortest distance between them.

In the phase $T_3 \in T$, as we mentioned before, a Type-B driver may be assigned either a ride-hailing request or an MST. The following inequality ensured that any Type-B driver could handle at most one sensing task or trip request simultaneously:

$$x^t_{dr} \leq 1 - x^t_{dk}, \quad \forall d, r, k \in \widetilde{\mathcal{D}}_t, \mathcal{R}_t, \mathcal{K}_T; \quad t \in T_3. \tag{3.17}$$

Here, $\widetilde{\mathcal{D}}_t$ represents the set of available Type-B vehicles in time period t, $\mathcal{R}_t$ denotes the set of available riders in time period t, and $\mathcal{K}_T$ indicates the set of MSTs released in the decision-making cycle T.

An auction venue will determine a winner if at least one driver's true valuation is collected. In mathematical terms, this condition can be expressed as:

$$\tau^t_k = 1, \quad \text{if} \quad \exists \delta^t_{dk} > -\infty, \ \forall k \in \mathcal{K}_T, \tag{3.18}$$

where τ^t_k is an indicator variable that equals 1 if the MST k is assigned to any driver, and 0 otherwise.

We present the following integer linear programming model to select the winners of the MSTs in the time period $t \in T_3$:

[MST-P1]

$$\max \quad \Pi = \sum_{k \in \mathcal{K}_T} \sum_{d \in \widetilde{\mathcal{D}}_t} \delta^t_{dk} x^t_{dk} \tag{3.19}$$

$$\text{s.t.} \quad \text{Eqs.}(3.15) - (3.18)$$

$$\sum_{k \in \mathcal{K}_T} x^t_{dk} \leq 1, \quad \forall d \in \widetilde{\mathcal{D}}_t \tag{3.20}$$

$$\sum_{d \in \widetilde{\mathcal{D}}_t} x^t_{dk} \leq 1, \quad \forall k \in \mathcal{K}_T \tag{3.21}$$

$$\sum_{d \in \widetilde{\mathcal{D}}_t} x^t_{dk} \geq \tau^t_k, \quad \forall k \in \mathcal{K}_T \tag{3.22}$$

$$x^t_{dk}, x^t_{dr}, \tau^t_k \in \{0, 1\} \tag{3.23}$$

In this formulation, Constraints (3.20) and (3.21) ensure that each driver or MST can be matched only once. Constraint (3.22) guarantees that any task request will be assigned when there are valid bidders for it.

As previously discussed, Type-B vehicles are considered to be 'redundant' vehicles if they fail to match any rider in phase T_1. These vehicles are eligible to participate in both the trip matching and MST assignment problems in phase T_3. To motivate Type-B drivers, the ride-hailing platform may prioritize MSTs in phase T_3. In other words, the MST assignment problem is solved first. Any unoccupied Type-A and Type-B drivers are subsequently matched to trip requests by addressing the trip matching problem, while those who win the auction are filtered out.

3.3.3 Payment determination

After assigning task requests to drivers, the next problem is to determine a final earning for each driver, which is calculated by the ride-hailing platform. A straightforward payment rule derives from the one-sided VCG mechanism. In the VCG-MST mechanism, the final earning of each driver d is determined by:

$$p^t_d = v^t_{dk} + (\Pi(\widetilde{\mathcal{D}}_t) - \Pi(\widetilde{\mathcal{D}}_t \setminus \{d\})) \quad \forall d \in \widetilde{\mathcal{D}}_t \tag{3.24}$$

where $\Pi(\widetilde{\mathcal{D}}_t)$ and $\Pi(\widetilde{\mathcal{D}}_t \setminus \{d\})$ represent the optimal objective function value with and without driver d. A driver's utility u^t_d is calculated as the difference between the earning and true valuation:

$$u^t_d = p^t_d - v^t_{dk} \tag{3.25}$$

Algorithm 2 summarizes the aforementioned winner selection and payment determination process, and shows how to implement the trip matching and task assignment in the phase T_3.

The VCG mechanism is proved to satisfy favorable economic properties such as Individual Rationality (IR), Allocative Efficiency (AE), and Incentive Compatibility (IC) (Krishna, 2009). In this study, the VCG-MST mechanism also satisfies these three properties.

Proposition 3.1. Individual Rationality *Any driver who bids an MST would not get a negative utility.*

Proof. From the Eq.(3.24) and Eq.(3.25), the driver's utility is $\Pi(\widetilde{\mathcal{D}}_t) - \Pi(\widetilde{\mathcal{D}}_t \setminus \{d\})$. If a driver d^* participates in sensing activity, the optimal value of $\sum_{k \in \mathcal{K}_T} \sum_{d \in \widetilde{\mathcal{D}}_t} \delta^t_{dk} x^t_{dk}$ is at least not less than that of $\sum_{k \in \mathcal{K}_T} \sum_{d \in \widetilde{\mathcal{D}}_t \setminus \{d^*\}} \delta^t_{dk} x^t_{dk}$, then we have $\Pi(\widetilde{\mathcal{D}}_t) \geq \Pi(\widetilde{\mathcal{D}}_t \setminus \{d^*\})$, which leads to $u^t_{d^*} \geq 0$. This completes the proof. □

Algorithm 2: Coordinating the VCG-MST assignment mechanism within trip matching

Input: The driver set $\mathcal{D}_t$, the task request set $\mathcal{K}_T$, the rider set $\mathcal{R}_t$, sensing cost saving matrix W

Output: Trip matching result $X_{\mathcal{DR}}$, MST assignment result $X_{\mathcal{WK}}$, vector of payments to MSTs $\mathbf{p}$

Solve the MST assignment model to obtain the optimal solution $X_{\mathcal{WK}}$, the set of winners $X_{\mathcal{W}}$ and the set of selected task requests $X_{\mathcal{K}}$;
Calculate the optimal objective function value $\Pi(\widetilde{\mathcal{D}}_t)$;
Solve the trip matching model to obtain the optimal solution $X_{\mathcal{DR}}$, the set of matched drivers $X_{\mathcal{D}}$ and the set of matched riders $X_{\mathcal{R}}$;
for $(d, r) \in X_{\mathcal{DR}}$ **do**
  if $d \in X_{\mathcal{W}}$ **then**
    Search for another idle driver d_2 who satisfies $d_2 = \arg\min_{j \in \mathcal{D}_t \setminus (X_{\mathcal{W}} \cup X_{\mathcal{D}})} \{L_{jr} \mid L_{jr} \leq L_{ub}\}$;
    if $\exists d_2 \in \mathcal{D}_t \setminus (X_{\mathcal{W}} \cup X_{\mathcal{D}})$ **then**
      replacing the incumbent driver d for rider r by d_2;
    else
      $X_{\mathcal{DR}} \leftarrow X_{\mathcal{DR}} \setminus \{(d, r)\}$, $X_{\mathcal{D}} \leftarrow X_{\mathcal{D}} \setminus \{d\}$, $X_{\mathcal{R}} \leftarrow X_{\mathcal{R}} \setminus \{r\}$;
for $d \in X_{\mathcal{W}}$ **do**
  Remove the row for driver d from the matrix W;
  Re-calibrate the MST assignment model to obtain the optimal objective function value $\Pi(\widetilde{\mathcal{D}}_t \setminus \{d\})$;
  Calculate the driver d's payoff $p_d^t = v_{dk}^t + (\Pi(\widetilde{\mathcal{D}}_t) - \Pi(\widetilde{\mathcal{D}}_t \setminus \{d\}))$;
Return $X_{\mathcal{DR}}, X_{\mathcal{WK}}, \mathbf{p}$

Proposition 3.2. Allocative Efficiency *When the model (3.19) achieves the optimal objective value, the VCG-MST auction mechanism for MST assignment achieves allocative efficiency.*

Proof. The objective function Eq.(3.19) aims to maximize the saving on sensing cost. In this MST problem, the VCG-MST auction mechanism operates as a price-only reverse auction, as it solely collects bidding information from participants. We let $\boldsymbol{x} = \{(i, j) \mid x_{ij} = 1\}$ be a feasible solution of the assignment model, and X be a set of all feasible solutions. If there exists an optimal solution $\boldsymbol{x}^*$ achieving $\boldsymbol{x}^* = \arg\max_{\boldsymbol{x} \in X} \sum_{k \in \mathcal{K}_T} \sum_{d \in \widetilde{\mathcal{D}}_t} \delta_{dk}^t x_{dk}^t$, the assignment result is efficient. In this problem, the model (3.19) is always trying to find the maximum objective value and optimal solution $\boldsymbol{x}^*$, indicating that allocative efficiency is achieved. □

Proposition 3.3. Incentive Compatibility *By the VCG-MST mechanism, submitting the true valuation to the platform is a dominant strategy for any driver despite how other drivers submit their bids.*

Proof. We assume that everyone in $\widetilde{\mathcal{D}}_t \setminus \{d\}$ submits price bidding truthfully. If driver d truthfully submits the price bidding $\mathcal{B}_d^t$, then the payoff is $p_d^t = v_{dk}^t + (\Pi(\widetilde{\mathcal{D}}_t) - \Pi(\widetilde{\mathcal{D}}_t \setminus \{d\}))$. If the driver d submits her bidding price $\hat{\mathcal{B}}_d^t \neq \mathcal{B}_d^t$ untruthfully, $\hat{v}_{dk}^t \neq v_{dk}^t$, then the payoff is $\hat{p}_d^t = \hat{v}_{dk}^t + (\hat{\Pi}(\widetilde{\mathcal{D}}_t) - \Pi(\widetilde{\mathcal{D}}_t \setminus \{d\}))$, and

$$\hat{\Pi}(\widetilde{\mathcal{D}}_t) = \hat{\delta}_{dk}^t + \sum_{j \in \mathcal{K}_t \setminus \{k\}} \sum_{l \in \widetilde{\mathcal{D}}_t \setminus \{d\}} \delta_{lj}^t x_{lj}^t$$

is the new objective function value. In light of the Cheng et al. (2023), we assume that driver d can be matched, and obtain a higher payoff by submitting untruthfully. Then, we have:

$$\hat{p}_d^t - v_{dk}^t > p_d^t - v_{dk}^t = \Pi(\widetilde{\mathcal{D}}_t) - \Pi(\widetilde{\mathcal{D}}_t \setminus \{d\}).$$

Substituting for $\hat{p}_d^t$ can get

$$
\begin{aligned}
& \hat{v}_{dk}^t + \hat{\Pi}(\widetilde{\mathcal{D}}_t) - \Pi(\widetilde{\mathcal{D}}_t \backslash \{d\}) - v_{dk}^t > \Pi(\widetilde{\mathcal{D}}_t) - \Pi(\widetilde{\mathcal{D}}_t \backslash \{d\}) \\
\Rightarrow \quad & \hat{v}_{dk}^t + \hat{\Pi}(\widetilde{\mathcal{D}}_t) - v_{dk}^t + c_q l_{qk} - c_q l_{qk} > \Pi(\widetilde{\mathcal{D}}_t) \\
\Leftrightarrow \quad & \delta_{dk}^t - \hat{\delta}_{dk}^t + \hat{\Pi}(\widetilde{\mathcal{D}}_t) > \Pi(\widetilde{\mathcal{D}}_t) \\
\Rightarrow \quad & \delta_{dk}^t - \hat{\delta}_{dk}^t + \hat{\delta}_{dk}^t + \sum_{j \in \mathcal{K}_T \backslash \{k\}} \sum_{l \in \widetilde{\mathcal{D}}_t \backslash \{d\}} \delta_{lj}^t x_{lj}^t > \Pi(\widetilde{\mathcal{D}}_t) \\
\Rightarrow \quad & \delta_{dk}^t + \sum_{j \in \mathcal{K}_T \backslash \{k\}} \sum_{l \in \widetilde{\mathcal{D}}_t \backslash \{d\}} \delta_{lj}^t x_{lj}^t > \Pi(\widetilde{\mathcal{D}}_t).
\end{aligned}
$$

This contradicts that the optimal objective value is $\Pi(\widetilde{\mathcal{D}}_t) = \sum_{j \in \mathcal{K}_T \backslash \{k\}} \sum_{l \in \widetilde{\mathcal{D}}_t \backslash \{d\}} \delta_{lj}^t x_{lj}^t + \delta_{dk}^t$, indicating that the driver d cannot obtain higher payoff by submitting untruthfully. Therefore, the VCG-MST auction mechanism satisfies incentive compatibility. □

4 A refine budget control mechanism for MST assignment

The VCG-based MST assignment mechanism offers a rational, efficient, and truthful approach to assigning MSTs within the ride-hailing platform. However, the resulting assignment plan may sometimes fail to meet budgetary requirements. Our numerical tests indicate instances where assigning MSTs to Type-B drivers proves to be more costly than utilizing dedicated vehicles for certain tasks. This could lead to budget deficit for the ride-hailing platform, thereby affecting the enthusiasm for incorporating mobile sensing services.

To address this challenge and maintain control over the overall budget, we propose a budget control mechanism for MST assignment, refining the winner determination and payment rule of the VCG mechanism. Moreover, the refined budget control MST assignment mechanism (RBC-MST) is also proved to satisfy some favorable economic properties.

4.1 Budget control for winner selection

The allocation of the mobile sensing budget directly impacts the sensing capabilities of the vehicles. A straightforward but potentially risky approach involves allocating the entire budget at once. Under this method, the budget for each cycle fluctuates throughout the decision-making process as payments from previous bidding rounds are subtracted. However, this approach may lead to substantial opportunity costs (Tafreshian and Masoud, 2022), particularly because complete information regarding the number and locations of MSTs may not be available initially.

An alternative strategy involves proportionally allocating the budget across each decision-making cycle for the MST assignment. After the assignment in each cycle is completed, the remaining fund for that cycle is returned back to a central budget pool. The amount of fund invested in each decision-making cycle is primarily determined by the numbers of sensing tasks released during that cycle and all unallocated sensing tasks. Subsequently, in each decision-making cycle, the RBC-MST mechanism determines the winners and payoffs for the current MST assignment based on the budget allocated to that cycle.

Let $\mathcal{K}_T^r$ denote the set comprising all unallocated sensing tasks up to the T-th decision-making cycle and $\mathcal{K}_T \subseteq \mathcal{K}_T^r$ be the subset of sensing tasks released in the decision-making cycle T. The partial budget Ω_T for this cycle T is then calculated by:

$$\Omega_T = \frac{|\mathcal{K}_T|}{|\mathcal{K}_T^r|}(\Omega - \sum_{i=0}^{T-1} \Theta_i) \tag{4.1}$$

where Ω is the total budget used for MST assignment, and Θ_i is the actual expense on sensing tasks in the decision-making cycle i and $\Theta_0 = 0$.

We are now ready to propose the following MST assignment problem by imposing an additional budget constraint while minimizing the total sensing cost in the time period $t \in T_3$.

[MST-P2]

$$\min \quad \Psi' = \sum_{k \in \mathcal{K}_T} \sum_{d \in \widetilde{\mathcal{D}}_t} v_{dk}^t x_{dk}^t \tag{4.2}$$

$$\text{s.t.} \quad \text{Eqs.(3.15), (3.17),(3.20)} - \text{(3.23)}$$

$$\tau_k^t = 1, \quad \exists v_{dk}^t < +\infty, \forall d \in \widetilde{\mathcal{D}}_t, k \in \mathcal{K}_T \tag{4.3}$$

$$\sum_{k \in \mathcal{K}_T} \sum_{d \in \widetilde{\mathcal{D}}_t} \overline{v}_{dk}^t x_{dk}^t \leq \Omega_T \tag{4.4}$$

Here, $\overline{v}_{dk}^t$ denotes the upper bound of driver d's true valuation when bidding to MST k. According to Equation (3.15), this upper bound depends on the relationship between the drivers maximum stated valuation and private valuation. Specifically:

- If the drivers maximum stated valuation exceeds the private valuation, we have $\overline{v}_{dk}^t = C + \overline{b} l_{dk}$.
- Otherwise, $\overline{v}_{dk}^t = \alpha l_{dk} + g(l_{dk})$.

However, imposing a budget constraint does not necessarily guarantee the feasibility of model [MST-P2], as in practical computation, it is possible to encounter situations where $\sum_{k \in \mathcal{K}_T} \sum_{d \in \widetilde{\mathcal{D}}_t} \overline{v}_{dk}^t x_{dk}^t > \Omega_T$, thereby violating the budget constraint (4.4).

To address this issue, we solve the model [MST-P2] directly without initially considering constraint (4.4). There are two cases to consider. In the first case, if the budget constraint (4.4) is verified to be feasible after solving the model, the solution can be accepted as optimal. In the second case, if the budget constraint is violated, the assignment result is adjusted to ensure compliance with the constraint. We will exclude the most "expensive" driver from the set, identified as the one with the largest true valuation. Let $\mathcal{WK}_t$ denote the tuple set of "winners" along with the MSTs assigned to them, then we have:

$$x_{l^* j^*}^t = 0, \quad (l^*, j^*) = \underset{(l,j) \in \mathcal{WK}_t}{\arg\max} \{ v_{lj}^t \mid \sum_{(l,j) \in \mathcal{WK}_t} \overline{v}_{lj}^t > \Omega_T \}. \tag{4.5}$$

The removed driver-MST pair is then added to a *tabu list* $\mathcal{NK}_t$, prohibiting its selection in future iterations. The [MST-P2] is then resolved with respect to the $\mathcal{NK}_t$. This procedure is iterated until the budget constraint is satisfied. If all drivers eligible for task k^* are in the tabu list, we may relax the constraint (4.3) based on the Equation (4.6).

$$\tau_{k^*}^t = \begin{cases} 1, & \text{if} \quad \exists v_{dk^*}^t < +\infty \text{ and } (d, k^*) \notin \mathcal{NK}_t, \forall d \in \widetilde{\mathcal{D}}_t \\ 0, & \text{others} \end{cases} \tag{4.6}$$

4.2 A tailored payment rule

As with the VCG-MST mechanism, we denote the set of successfully matched driver-task pairs as $\mathcal{WK}_t$, with $\mathcal{W}_t$ representing the set of winners and $\mathcal{K}_t$ representing the set of task requests. We propose the following payment rule for the selected drivers. Driver d's payoff is determined by:

$$p_d^t = \begin{cases} \overline{v}_{dk}^t, & \Psi'(\widetilde{\mathcal{D}}_t \backslash \{d\}) < \Psi'(\widetilde{\mathcal{D}}_t) \\ \min \left\{ v_{dk}^t + \left(\Psi'(\widetilde{\mathcal{D}}_t \backslash \{d\}) - \Psi'(\widetilde{\mathcal{D}}_t) \right), \ \overline{v}_{dk}^t \right\}, & \Psi'(\widetilde{\mathcal{D}}_t \backslash \{d\}) \geq \Psi'(\widetilde{\mathcal{D}}_t) \end{cases} \tag{4.7}$$

Assuming that $X(\widetilde{\mathcal{D}}_t \backslash \{d\})$ and $X(\widetilde{\mathcal{D}}_t)$ are solutions corresponding to the optimal objective value $\Psi'(\widetilde{\mathcal{D}}_t \backslash \{d\})$ and $\Psi'(\widetilde{\mathcal{D}}_t)$, respectively. We also utilize the marginal benefit of the winner d to calculate his/her payoff, but this payoff can not exceed the upper bound of d's true valuation. It is worth noting that the number of driver-MST pairs in $X(\widetilde{\mathcal{D}}_t \backslash \{d\})$ is less than that in $X(\widetilde{\mathcal{D}}_t)$ when the inequality $\Psi'(\widetilde{\mathcal{D}}_t \backslash \{d\}) < \Psi'(\widetilde{\mathcal{D}}_t)$ holds. This is because the task k can not be assigned when excluding the driver d from $\widetilde{\mathcal{D}}_t$. There are two cases leading to this result, i.e., (1) driver d is the only eligible bidder for the task k; (2) all driver-MST pairs to the task k are prohibited except for the driver d when solving the model [MST-P2]. In this situation, we set the upper bound of the driver's true valuation as the payoff.

The whole process is summarized in Algorithm 3.

Algorithm 3: Coordinating the RBC-MST assignment mechanism within trip matching

---

Input: The driver set $\mathcal{D}_t$, the MST set $\mathcal{K}_T$, the rider set $\mathcal{R}_t$, the true valuation matrix V, the budget Ω_T

Output: Trip matching result $X_{\mathcal{DR}}$, task assignment result $X_{\mathcal{WK}}$, task payment $\mathbf{p}$

$\mathcal{NK}_t, X_{\mathcal{WK}}, X_{\mathcal{W}}, X_{\mathcal{K}} \leftarrow \varnothing$;
$flag \leftarrow$ **True**;
while *flag* **do**
  Solve the [MST-P2] without considering budget constraint to obtain the optimal solution $\mathcal{WK}_t$, the set of winners $\mathcal{W}_t$ and the set of selected task requests $\mathcal{K}_t$;
  if $\sum_{(d,k)\in \mathcal{WK}_t} \overline{v}^t_{dk} > \Omega_T$ **then**
    $d^*, k^* = \arg\max_{(d,k)\in\mathcal{WK}_t} \{v^t_{dk}\}$;
    if $\forall (d, k^*) \in \mathcal{NK}_t$ and $v^t_{dk^*} < +\infty$ **then**
      $\tau^t_{k^*} \leftarrow 0$;
    $\mathcal{NK}_t \leftarrow \mathcal{NK}_t \cup \{(d^*, k^*)\}$;
  else
    $X_{\mathcal{WK}} \leftarrow \mathcal{WK}_t$, $X_{\mathcal{W}} \leftarrow \mathcal{W}_t$, $X_{\mathcal{K}} \leftarrow \mathcal{K}_t$;
    $flag \leftarrow$ **False**;
Find the optimal solution $X_{\mathcal{DR}}$ following the steps 3 to 10 of Algorithm 2;
for $(d,k) \in X_{\mathcal{WK}}$ **do**
  Re-calibrate the MST assignment model to obtain the optimal objective function value $\Psi'(\widetilde{D}_t \backslash \{d\})$ without considering the driver d;
  Calculate the driver d's payoff based on the tailored payment rule;
Return $X_{\mathcal{DR}}, X_{\mathcal{WK}}, \mathbf{p}$

4.3 An illustrative example

In this subsection, we intend to use an illustrative example to simply clarify how to solve MST assignment problem by using [MST-P2]. We assume that, in a time period $t \in T_3$, there are four drivers and three unallocated sensing tasks in current matching pool. Let $\widetilde{\mathcal{D}}_t = \{d_1, d_2, d_3, d_4\}$ and $\mathcal{K}_T = \{k_1, k_2, k_3\}$ be the set of drivers and the set of sensing tasks, respectively. We randomly generate some true valuations and their upper bounds, which will be used in model, and we assume the platform needs to determine the assignment result based on the following matrix:

$$\mathrm{V} = \begin{bmatrix} 20 & 9 & +\infty \\ +\infty & 10 & 13 \\ +\infty & 8 & 15 \\ +\infty & +\infty & 10 \end{bmatrix}, \quad \overline{\mathrm{V}} = \begin{bmatrix} 22 & 10 & +\infty \\ +\infty & 12 & 15 \\ +\infty & 10 & 17 \\ +\infty & +\infty & 14 \end{bmatrix}$$

where V is a matrix of true valuations and $\overline{\mathrm{V}}$ is a matrix of upper bounds of the true valuations. It should be noting that only driver d_1 bids for MST k_1. According to our model, the MST

k_1 must be assigned to the driver d_1 due to the constraint (4.3).

When we do not consider the budget constraint (4.4), the optimal objective value and solution are $\Psi'_{min} = 20+8+10 = 38$ and $\mathcal{WK}_t = \{(1,1),(3,2),(4,3)\}$, respectively. Then, we will consider two cases where the partial budget Ω_T is equal to 50 or 40.

Case 1: $\Omega_T = 50$. In this case, the budget constraint is verified to be feasible due to $\sum_{(l,j)\in\mathcal{WK}_t} \overline{v}^t_{dk} = \overline{v}_{11} + \overline{v}_{32} + \overline{v}_{43} = 22+10+14 = 46 < 50$. This solution is accepted as optimal, and we then calculate each winner's final earning based on the Equation (4.7):

- For winner d_1, we find the minimum $\Psi'(\widetilde{\mathcal{D}}_t \backslash \{d_1\}) = 18 < \Psi'(\widetilde{\mathcal{D}}_t) = 38$ because only driver 1 bids for MST 1. Then, this driver's final earning is the upper bound of the true valuation $p_1 = \overline{v}_{11} = 22$.
- For winner d_3, the minimum $\Psi'(\widetilde{\mathcal{D}}_t \backslash \{d_3\}) = 40 > \Psi'(\widetilde{\mathcal{D}}_t) = 38$, then the final earning is $p_3 = \min\left\{v_{32} + (\Psi'(\widetilde{\mathcal{D}}_t \backslash \{d_3\}) - \Psi'(\widetilde{\mathcal{D}}_t)), \overline{v}_{32}\right\} = \min\{8+(40-38), 10\} = 10$.
- For winner d_4, the minimum $\Psi'(\widetilde{\mathcal{D}}_t \backslash \{d_4\}) = 41 > \Psi'(\widetilde{\mathcal{D}}_t) = 38$, then the final earning is $p_4 = \min\left\{v_{43} + (\Psi'(\widetilde{\mathcal{D}}_t \backslash \{d_4\}) - \Psi'(\widetilde{\mathcal{D}}_t)), \overline{v}_{43}\right\} = \min\{10+(41-38), 14\} = 13$.

Case 2: $\Omega_T = 40$. In this case, the budget constraint is verified to be infeasible at the first time due to $\sum_{(l,j)\in\mathcal{WK}_t} \overline{v}^t_{dk} = \overline{v}_{11} + \overline{v}_{32} + \overline{v}_{43} = 22+10+14 = 46 > 40$. Then, based on the Equation (4.5), we let $x_{11} = 0$ and $\mathcal{NK}_t = \{(1,1)\}$. In addition, according to Equation (4.6), τ^t_1 must be equal to 0 after adding $x_{11} = 0$ into the model [MST-P2] because conditions $(1,1) \in \mathcal{NK}_t, v_{21} = v_{31} = v_{41} = +\infty$ hold.

When solving the [MST-P2] again with the new constraint $x_{11} = 0$, we obtain the optimal solution and the budget constraint is verified to be feasible. The optimal objective value and solution are $\Psi'_{min} = 8+10 = 18$ and $\mathcal{WK}_t = \{(3,2),(4,3)\}$, respectively. Moreover, $\sum_{(l,j)\in\mathcal{WK}_t} \overline{v}^t_{dk} = \overline{v}_{32} + \overline{v}_{43} = 10+14 = 24 < 40$. This solution is accepted as optimal, and we then calculate each winner's final earning based on the Equation (4.7):

- For winner d_3, the minimum $\Psi'(\widetilde{\mathcal{D}}_t \backslash \{d_3\}) = 19 > \Psi'(\widetilde{\mathcal{D}}_t) = 18$, then the final earning is $p_3 = \min\left\{v_{32} + (\Psi'(\widetilde{\mathcal{D}}_t \backslash \{d_3\}) - \Psi'(\widetilde{\mathcal{D}}_t)), \overline{v}_{32}\right\} = \min\{8+(19-18), 10\} = 9$.
- For winner d_4, the minimum $\Psi'(\widetilde{\mathcal{D}}_t \backslash \{d_4\}) = 21 > \Psi'(\widetilde{\mathcal{D}}_t) = 18$, then the final earning is $p_4 = \min\left\{v_{43} + (\Psi'(\widetilde{\mathcal{D}}_t \backslash \{d_4\}) - \Psi'(\widetilde{\mathcal{D}}_t)), \overline{v}_{43}\right\} = \min\{10+(21-18), 14\} = 13$.

4.4 Economic properties of RBC-MST mechanism

While the VCG-MST mechanism has some favorable properties, it generally does not meet an important property called "budget balance". In fact, our proposed RBC-MST mechanism can handle this problem well, though it may sacrifice the "allocative efficiency" because efficient assignment results may be changed with the introduction of budget constraints. Previous study has shown that no such mechanism can simultaneously satisfy the individual rationality (IR), incentive compatibility (IC), allocative efficiency (AE) and budget balance (BB) (Krishna, 2009). In the RBC-MST mechanism, we attempt to prove that the mechanism satisfies IR, IC, and BB. These properties ensure that drivers benefit from serving sensing tasks, remain truthful in auction bidding, and that the budget provided to the ride-hailing platform remains non-negative. Establishing these three economic properties highlights the strong practical applicability of the proposed mechanism.

The proposed RBC-MST mechanism is proved to satisfy BB, IC, and IR properties. Additionally, under the condition of prohibiting driver-MST pairs in the tabu list $\mathcal{NK}_t$ (e.g., $\mathcal{NK}_t = \emptyset$), RBC-MST mechanism achieves the efficient allocation. Before proving the BB property, we show the assignment mechanism satisfies Lemma 1.

Lemma 1. *For any valid true valuation submitted by a driver $d \in \widetilde{\mathcal{D}}_t$, $\overline{v}_{dk}^t$ is always greater than or equal to v_{dk}^t.*

Proof. Based on the Equation (3.15), there are two cases to consider.

(1) In the first one, we let $v_{dk}^t = C + \mathcal{B}_d^t l_{dk} > \alpha l_{dk} + g(l_{dk})$, indicating that the driver d submits the true valuation corresponding to the stated valuation. Then, according to (3.13), we have $v_{dk}^t = C + \mathcal{B}_d^t l_{dk} \leq C + \overline{b} l_{dk} = \overline{v}_{dk}$.

(2) In the second one, we let $v_{dk}^t = \alpha l_{dk} + g(l_{dk}) = (\alpha+\mu) l_{dk} - \mu l_0 + f_m + \xi \geq C + \mathcal{B}_d^t l_{dk}$, indicating that the driver d submits the true valuation corresponding to the private valuation. If $l_{dk} \geq \frac{C+\mu l_0 - f_m - \xi}{\alpha+\mu-\overline{b}}$, we have $C + \overline{b} l_{dk} \leq (\alpha+\mu) l_{dk} - \mu l_0 + f_m + \xi$. According to the definition of $\overline{v}_{dk}^t$ in the model [MST-P2], when $C + \overline{b} l_{dk} \leq (\alpha+\mu) l_{dk} - \mu l_0 + f_m + \xi$, we can obtain $\overline{v}_{dk}^t = (\alpha+\mu) l_{dk} - \mu l_0 + f_m + \xi$. Hence, $\overline{v}_{dk}^t$ is equal to v_{dk}^t. If $l_{dk} < \frac{C+\mu l_0 - f_m - \xi}{\alpha+\mu-\overline{b}}$, we have $C + \overline{b} l_{dk} > (\alpha+\mu) l_{dk} - \mu l_0 + f_m + \xi$. Similarly, we can obtain $\overline{v}_{dk}^t = C + \overline{b} l_{dk} > (\alpha+\mu) l_{dk} - \mu l_0 + f_m + \xi = v_{dk}^t$.

In both cases, $\overline{v}_{dk}^t \geq v_{dk}^t$. This completes the proof. □

Proposition 4.1. Budget Balance *In each plan cycle, the actual expenditure incurred by the RBC-MST mechanism is either less than or equal to the prescribed budget Ω_T.*

Proof. Let the driver d's true valuation be $v_{dk}^t = \max\left\{C + \mathcal{B}_{dk}^t l_{dk}, \alpha l_{dk} + g(l_{dk})\right\}$ at the optimal solution $\mathcal{WK}_t$. With Lemma 1, $\overline{v}_{dk}^t \geq v_{dk}^t$ always holds. Therefore $\overline{v}_{dk}^t$ is the upper bound of the driver d's true valuation.

By Equation (4.7), the actual payments satisfies:

$$\sum_{(d,k)\in\mathcal{WK}_t} v_{dk}^t \leq \sum_{(d,k)\in\mathcal{WK}_t} p_d^t \leq \sum_{(d,k)\in\mathcal{WK}_t} \overline{v}_{dk}^t.$$

Due to the constraints in [MST-P2], the true valuation of the selected winners satisfies $\sum_{(d,k)\in\mathcal{WK}_t} \overline{v}_{dk}^t \leq \Omega_T$. Thus, we obtain

$$\sum_{(d,k)\in\mathcal{WK}_t} p_d^t \leq \sum_{(d,k)\in\mathcal{WK}_t} \overline{v}_{dk}^t \leq \Omega_T.$$

Thus, the actual payment in any decision-making cycle T is less than or equal to the budget Ω_T. □

Proposition 4.2. Individual Rationality *With the RBC-MST mechanism, every eligible driver who submits bids will not incur negative utility.*

Proof. Let $\Psi_{\mathcal{WK}_t}$ to be the corresponding value of the objective function of [MST-P2]. For any driver-MST pair $(d,k) \in \mathcal{WK}_t$, we have $x_{dk}^t = 1$.

When $\Psi'(\widetilde{\mathcal{D}}_t \backslash \{d\}) \geq \Psi'(\widetilde{\mathcal{D}}_t)$, the utility of driver d satisfies

$$\begin{aligned} u_d^t = p_d^t - v_{dk}^t &= \min\left\{v_{dk}^t + \left(\Psi'(\widetilde{\mathcal{D}}_t \backslash \{d\}) - \Psi'(\widetilde{\mathcal{D}}_t)\right),\ \overline{v}_{dk}^t\right\} - v_{dk}^t \\ &= \min\left\{\left(\Psi'(\widetilde{\mathcal{D}}_t \backslash \{d\}) - \Psi'(\widetilde{\mathcal{D}}_t)\right),\ \overline{v}_{dk}^t - v_{dk}^t\right\} \geq 0. \end{aligned}$$

When $\Psi'(\widetilde{\mathcal{D}}_t \backslash \{d\}) < \Psi'(\widetilde{\mathcal{D}}_t)$, we have $p_d^t - v_{dk}^t = \overline{v}_{dk}^t - v_{dk}^t \geq 0$ by Lemma 1.

Therefore, each selected driver can attain non-negative utility, while the utility of any deselected driver is null. This completes the proof of the IR property. □

Proposition 4.3. Incentive Compatibility *Submitting a truthful bid is a dominant strategy for any driver in the RBC-MST mechanism given the other drivers submit truthful bids.*

Proof. We may discuss a driver's change in utility when submitting an untruthful bid. A driver may be (1) selected, or (2) deselected for any MSTs when submits a bid truthfully.

By Equation (4.7), there are three cases of the payment to any selected driver. The utility in submitting an untruthful bid may also evaluated accordingly.

(1) $\Psi'(\widetilde{\mathcal{D}}_t\backslash\{d\}) < \Psi'(\widetilde{\mathcal{D}}_t)$. This case occurs only when any valid match pairs for the sensing task k are in the tabu list. If d is excluded, the sensing task k may be left unassigned. In this case, the driver d will obtain the upper bound of the own true valuation despite the bid. Thus, driver d's utility remains the same.

(2) $\Psi'(\widetilde{\mathcal{D}}_t\backslash\{d\}) \geq \Psi'(\widetilde{\mathcal{D}}_t)$ and $\Psi'(\widetilde{\mathcal{D}}_t\backslash\{d\}) - \Psi'(\widetilde{\mathcal{D}}_t) > \overline{v}^t_{dk} - v^t_{dk}$. It means that the marginal benefit of the driver d is above the valuation the upper bound of valuation minus true valuation. The driver d who is selected will obtain the upper bound of the own true valuation. In this case, the utility of driver d remains the same.

(3) $\Psi'(\widetilde{\mathcal{D}}_t\backslash\{d\}) \geq \Psi'(\widetilde{\mathcal{D}}_t)$ and $\Psi'(\widetilde{\mathcal{D}}_t\backslash\{d\}) - \Psi'(\widetilde{\mathcal{D}}_t) \leq \overline{v}^t_{dk} - v^t_{dk}$. Assuming that the driver d can obtain higher payoff $\hat{p}^t_d$ by untruthful submission. Then, we have:

$$\hat{p}^t_d - v^t_{dk} > p^t_d - v^t_{dk} = \Psi'(\widetilde{D}_t\backslash\{d\}) - \Psi'(\widetilde{D}_t)$$

Substituting $\hat{p}^t_d = \hat{v}^t_{dk} + \big(\Psi'(\widetilde{\mathcal{D}}_t\backslash\{d\}) - \hat{\Psi}'(\widetilde{\mathcal{D}}_t)\big)$ into above inequality, we get:

$$\begin{aligned}
& \hat{v}^t_{dk} + \big(\Psi'(\widetilde{\mathcal{D}}_t\backslash\{d\}) - \hat{\Psi}'(\widetilde{\mathcal{D}}_t)\big) - v^t_{dk} > \Psi'(\widetilde{\mathcal{D}}_t\backslash\{d\}) - \Psi'(\widetilde{\mathcal{D}}_t) \\
\Rightarrow\quad & \hat{v}^t_{dk} - \hat{\Psi}'(\widetilde{\mathcal{D}}_t) - v^t_{dk} > -\Psi'(\widetilde{\mathcal{D}}_t) \\
\Rightarrow\quad & \hat{\Psi}'(\widetilde{\mathcal{D}}_t) + v^t_{dk} - \hat{v}^t_{dk} < \Psi'(\widetilde{\mathcal{D}}_t) \\
\Leftrightarrow\quad & \hat{v}^t_{dk} + \sum_{j\in\mathcal{K}_T\backslash\{k\}} \sum_{l\in\widetilde{\mathcal{D}}_t\backslash\{d\}} v^t_{lj}x^t_{lj} + v^t_{dk} - \hat{v}^t_{dk} < \Psi'(\widetilde{\mathcal{D}}_t) \\
\Rightarrow\quad & v^t_{dk} + \sum_{j\in\mathcal{K}_T\backslash\{k\}} \sum_{l\in\widetilde{\mathcal{D}}_t\backslash\{d\}} v^t_{lj}x^t_{lj} < \Psi'(\widetilde{\mathcal{D}}_t)
\end{aligned}$$

It contradicts that $\Psi'(\widetilde{\mathcal{D}}_t) = v^t_{dk} + \sum_{j\in\mathcal{K}_T\backslash\{k\}} \sum_{l\in\widetilde{\mathcal{D}}_t\backslash\{d\}} v^t_{lj}x^t_{lj}$ is optimal objective value. Therefore, the utility of any selected driver d can not increase by untruthful bidding.

We may now discuss the utility change of any deselected driver when submits an untruthful bid. There are two cases for these drivers.

(1) When the driver d overbids, the valuations to all tasks increase. The optimal driver-MST pairs remain unchanged, which means that the driver d is still deselected. In this case, the utility of driver d remains zero.

(2) When the driver d underbids, the valuations to all tasks decrease. As the bid continuously decreases, d may take over task k from the initially assigned driver l, whose valuation to the task is v^t_{lk}. Let $v^t_{dk}, \hat{v}^t_{dk}$ denote driver d's true valuation and false valuation to task k, respectively. When $\hat{v}^t_{dk} > v^t_{lk}$, the driver d is still not selected and the utility remains the same. When $\hat{v}^t_{dk} \leq v^t_{lk}$, d replaces l as the selected driver, and we have $\hat{v}^t_{dk} \leq v^t_{lk} \leq v^t_{dk} \leq \overline{v}^t_{dk}$. Let the sum of the other driver-MST pairs' true valuations be $\mathit{\Psi}_{-k}$. Then d's payoff could be calculated by Equation (4.7):

$$\begin{aligned}
\hat{p}_d &= \min\left\{\hat{v}^t_{dk} + \big(\hat{\Psi}'(\widetilde{D}_t\backslash\{d\}) - \hat{\Psi}'(\widetilde{D}_t)\big), \overline{v}^t_{dk}\right\} \\
&= \min\left\{\hat{v}^t_{dk} + \big(v^t_{lk} + \mathit{\Psi}_{-k} - (\hat{v}^t_{dk} + \mathit{\Psi}_{-k})\big), \overline{v}^t_{dk}\right\} = \min\left\{v^t_{lk}, \overline{v}^t_{dk}\right\} = v^t_{lk} \leq v^t_{dk}
\end{aligned}$$

The payoff of driver d is less than the own true valuation v^t_{dk} when submitting untruthfully. In this case, the utility of driver d is negative.

Thus, submitting truthfully to the platform is a dominant strategy for either a selected or a deselected driver. This completes the proof. $\square$

5 Computational experiments

We conducted numerical tests using a large-scale instance generated from New York City taxi data. Initially, we assessed the performance of both the VCG-MST and RBC-MST mechanisms across various scenarios. Following this, we examined how taxi fleet size and the ratio between the two types of taxis impact the completion rate of sensing tasks. Lastly, we investigated the average payoffs for both Type-A and Type-B drivers under different bidding bounds, aiming to determine the willingness of Type-B drivers to undertake MSTs.

All algorithms presented in this article were implemented in Python 3.10, and integer programming problems were solved using Gurobi 10.0.0.

5.1 Description of experimental data and parameter settings

We chose the Manhattan borough of New York City as the testing area for our numerical experiments. Taking advantage of yellow taxi trip records from January 3rd to January 6th, 2022, sourced from the NYC Taxi and Limousine Commission (TLC) (NYC Taxi and Limousine Commission, 2022), we inferred estimated cruising times for calculating opportunity costs in the trip matching process. To assess the performance of the proposed mechanisms, we employed trip records from January 7th, 2022, spanning two hours.

To simplify calculations, we converted the area IDs of pick-up and drop-off locations for each trip record into network node IDs corresponding to the respective area. To test the performance of mechanisms under different trip demand scenarios, we extracted low trip demand scenarios (1,000 trip requests during the time horizon) and high trip demand scenarios (2,000 trip requests during the time horizon) from the raw data using standard sampling techniques. It is worth noting that the extracted trip requests is a subset of the actual trip requests. Meanwhile, we computed the average origin-destination (OD) distance for all trip requests. The value is around 3km. Thus, we set $l_0 \approx 3$ km.

The overall time horizon was set to 2 hours. Type-A taxi operations were scheduled every 30 seconds, while Type-B taxi planning cycles were set at 5 minutes. Each cycle was divided into 3 phases as described in Section 3: ride-hailing task matching T_1, mobile sensing task bidding T_2, and mobile sensing task assignment T_3. The durations of these phases were 3 minutes, 1.5 minutes, and 30 seconds, respectively.

We randomly selected the locations of 80 MSTs within the study area. Figure 5 displays the heat map of trip demand scenarios and the locations of MSTs within the Manhattan road network. Additionally, we randomly placed the depot of dedicated vehicles within the area to facilitate distance calculations between the dedicated vehicles and the MSTs. Furthermore, in our experiment, we let the service time be $t_s = 2.5$ minutes when a Type-B driver arrives at a PoI marked on the MST. We can roughly estimate the constant time cost in executing sensing task $\xi \approx \alpha \overline{V} t_s = 2 \times 35 \times \frac{2.5\times 60}{3600} = 2.92$. Table 2 shows other parameter values.

Table 2: Values of parameters

Parameters	Values	Parameters	Values
p_r^s	12 units	α	2 units/km
β_1	1.70 units/km	$\underline{b}$	2 units/km
β_2	0.50 units/min	$\overline{b}$	4 units/km
L_0^s	3 km	μ	1 unit/km
t_0^s	10 min	c_q	8 units/km
L_{ub}	2 km	C	15 units
$\overline{V}$	35 km/h	l_0	3 km
f_m	7.5 units		

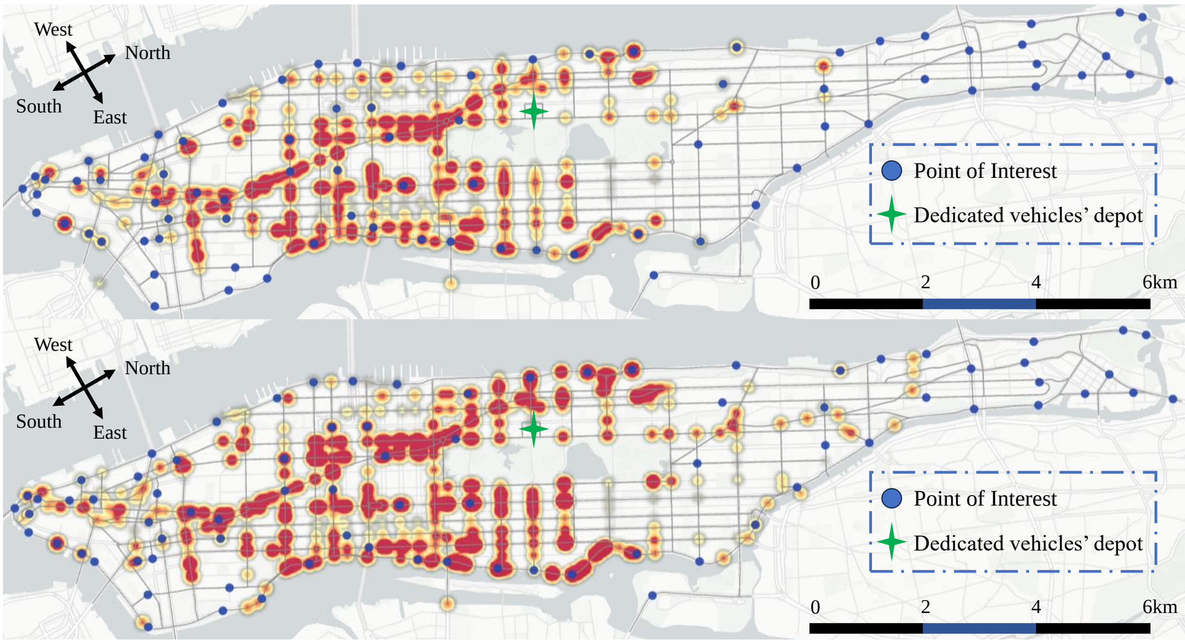

Figure 5: The low trip demand scenario, the high trip demand scenario and the locations of selected PoIs.

5.2 Performance of the VCG-MST and RBC-MST under different travel demands

We begin by evaluating the performance of the two mechanisms under different levels of travel demand. The total number of vehicles remains fixed at 140, while the ratio between the two types of vehicles varies across the tests. After executing the coordination strategy, three key indices are calculated: the social surplus, the remaining budget, and the completion rate of MSTs by taxis.

In this study, we define the social surplus as the difference between the total fixed cost of using dedicated vehicles to complete tasks and the total expense on sensing tasks. Essentially, it reflects the combined interests of the data user and the ride-hailing platform. For data user, social surplus directly represents the reduction in sensing cost that data user can achieve. For ride-hailing platform, social surplus indirectly reflects the potential benefit it can derive from collaborating with the data user. In other words, achieving higher social surplus benefits both parties, which necessitates reducing sensing cost to accomplish. The social surplus (SS) can be calculated as follows:

$$SS = \sum_{T \in \mathcal{T}} \sum_{(d,k) \in \mathcal{WK}_T} (c_q l_{qk} - p_{dk}^T), \tag{5.1}$$

where $c_q l_{qk}$ denotes the fixed cost of utilizing a dedicated vehicle to complete the sensing task k, and p_{dk}^T represents the expense by assigning the sensing task k to driver d during the decision-making cycle T.

The remaining budget quantifies the deficit or revenue of the ride-hailing platform in the MST business. Let RB represent the remaining budget at the end of the time horizon, and Ω be the initial budget provided in advance. RB can be calculated as follows:

$$RB = \Omega - \sum_{T \in \mathcal{T}} \sum_{(d,k) \in \mathcal{WK}_T} p_{dk}^T. \tag{5.2}$$

The completion rate of MSTs by taxis gauges the appeal of taxi-based mobile sensing to the data user, indicating the extent to which the taxi fleet can substitute dedicated vehicles. Let CR represent the completion rate of MSTs, $|\mathcal{WK}_T|$ denote the number of task requests assigned to drivers in decision-making cycle T, and $|\mathcal{K}|$ denote the total number of MSTs. CR can be calculated as follows:

$$CR = \frac{\sum_{T\in\mathcal{T}}|\mathcal{WK}_T|}{|\mathcal{K}|}. \tag{5.3}$$

Due to the random nature of the inputs, we conducted 5 repeated experiments for both the low-demand and high-demand cases, calculating the average of each index. Figure 6 compares the performance of the two MST assignment mechanisms under the low trip demand scenario. It's notable that the RBC-MST mechanism outperforms the VCG-MST mechanism in terms of social surplus (SS) and remaining budget (RB), but performs slightly worse than the VCG-MST mechanism in completion rate (CR). This discrepancy arises from the allocation rules of the two mechanisms.

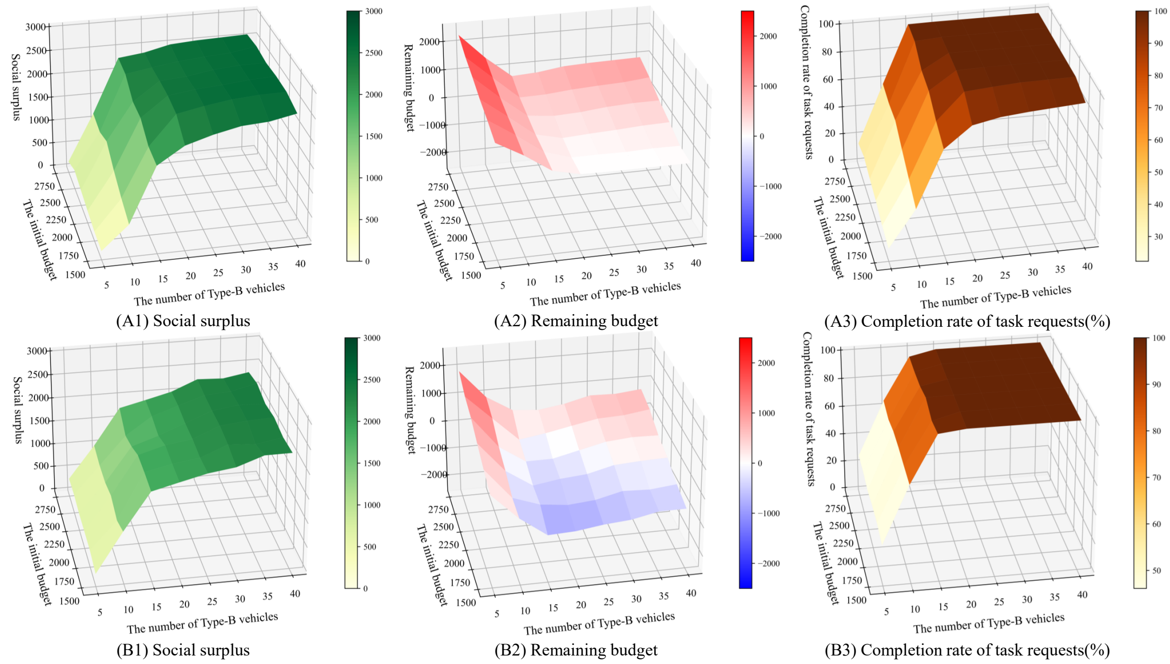

(A1) Social surplus (A2) Remaining budget (A3) Completion rate of task requests(%)

(B1) Social surplus (B2) Remaining budget (B3) Completion rate of task requests(%)

Figure 6: Comparison of (A) RBC-MST and (B) VCG-MST mechanism under the low trip demand scenario

The RBC-MST mechanism regulates the number of MSTs commissioned in each planning cycle based on the allocated budget. Consequently, some tasks, which might not be economically viable for the ride-hailing platform upon initial release, are deferred and assigned to drivers in subsequent auctions. This approach enables the platform to generate more social surplus and maintain a higher remaining budget. On the contrary, the VCG-MST mechanism assigns MSTs to drivers as long as their contributions to the objective are positive, following a greedier approach. While this approach results in a higher task completion rate, it may lead to excessive expenses on specific MSTs, potentially causing a deficit.

From Figure 6, we observe that the RBC-MST mechanism operates optimally when the taxi fleet consists of 20 Type-B vehicles and 120 Type-A vehicles in this low trip demand scenario. Under these conditions, both the social surplus and completion rate reach their maximum, and the remaining budget remains non-negative.

Similar numerical experiments were conducted for the high trip demand scenario, and the results of the RBC-MST and VCG-MST mechanisms are summarized in Figure 7. Notably, there are no significant differences between these two mechanisms across all three indices, although the RBC-MST mechanism performs slightly better in terms of social surplus and remaining budget, but slightly worse in completion rate. This observation can be attributed to the fact that when travel demand is high, most Type-A and Type-B vehicles are allocated to trip requests rather than MSTs.

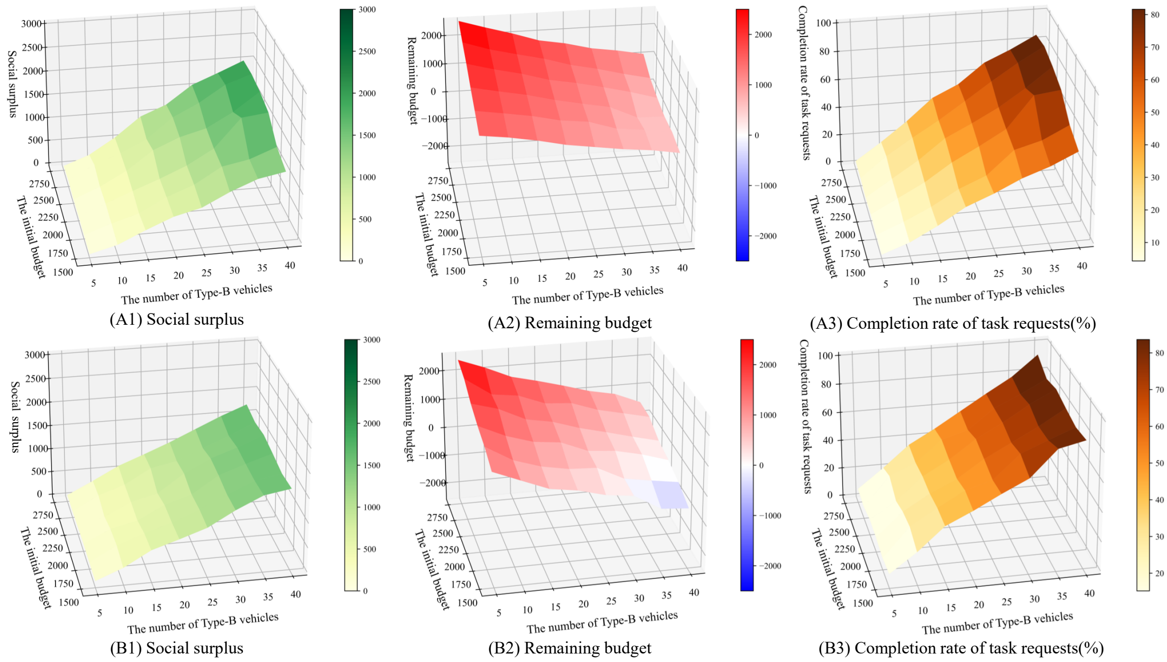

Figure 7: Comparison of (A) RBC-MST and (B) VCG-MST mechanism under the high trip demand scenario

5.3 Impact of the vehicle fleet sizes

In this subsection, we investigate the impact of taxi fleet sizes on the performance of the two mechanisms. We measure the service level for riders by calculating the average trip matching rate and average waiting time. Additionally, we evaluate the effectiveness of the coordinated strategy for mobile sensing using the social surplus and the completion rate of MSTs. For these experiments, we employ 20 Type-B vehicles in the taxi network, while the number of Type-A vehicles range from 40 to 160 with a step size of 20. Each experiment is repeated 5 times, and the average value of each index is calculated and presented in Figure 8. It's observed that the trip matching rate generally increases and the average waiting time of riders decreases with the increase in the number of Type-A vehicles. Furthermore, both mechanisms provide great service level of trip matching as the size of vehicle fleet increases.

Figure 9 illustrates the impact of the number of Type-A vehicles on the performances of the MST assignment. In scenarios with low travel demand, the social surplus increases with the number of available vehicles for both MST assignment mechanisms. However, this increase plateaus when the number of Type-A vehicles reaches around 100, indicating that all sensing tasks could be efficiently commissioned to the Type-B vehicles. Notably, the RBC-MST mechanism consistently yields a larger social surplus than the VCG-MST mechanism when the number of Type-A vehicles is not less than 60, making it particularly attractive to both the data user and the ride-hailing platform.

While a similar increasing pattern of the social surplus is observed in scenarios with high travel demand, no mechanism demonstrates consistently superior performance across all tests. The VCG-MST mechanism achieves a higher completion rate than the RBC-MST mechanism.

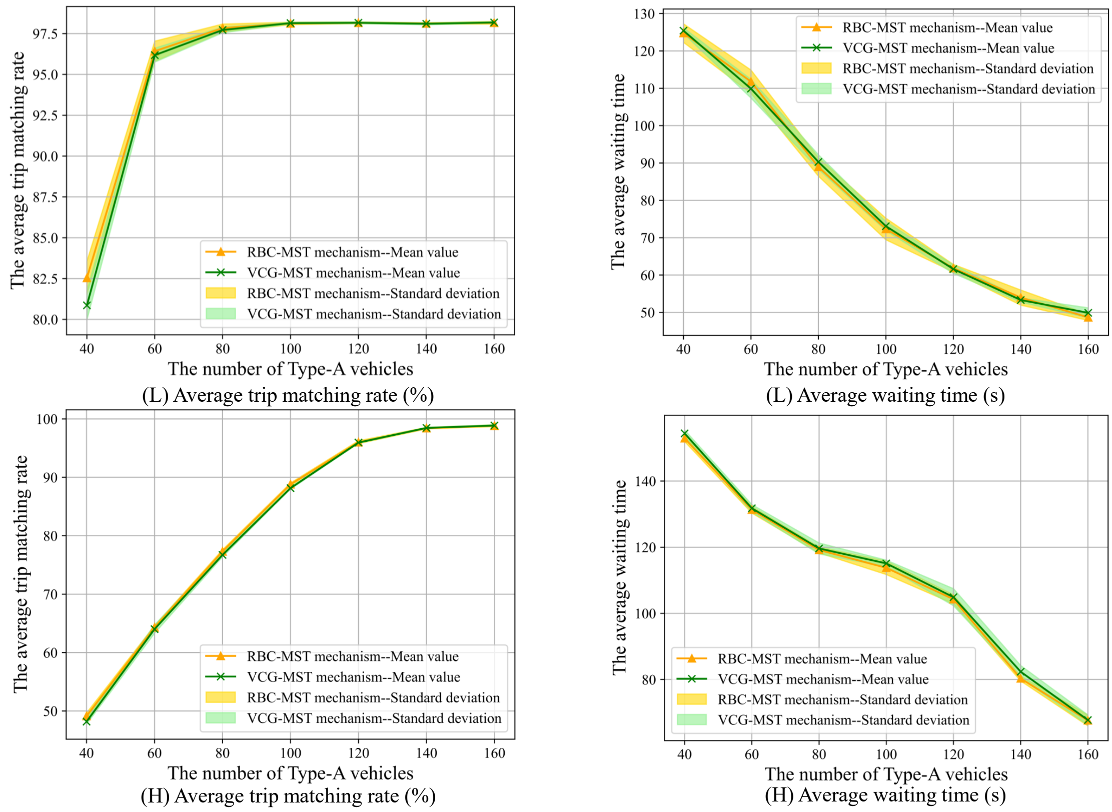

Figure 8: The impact of the various number of Type-A vehicles on trip matching in (L) low travel demand scenario and (H) high travel demand scenario

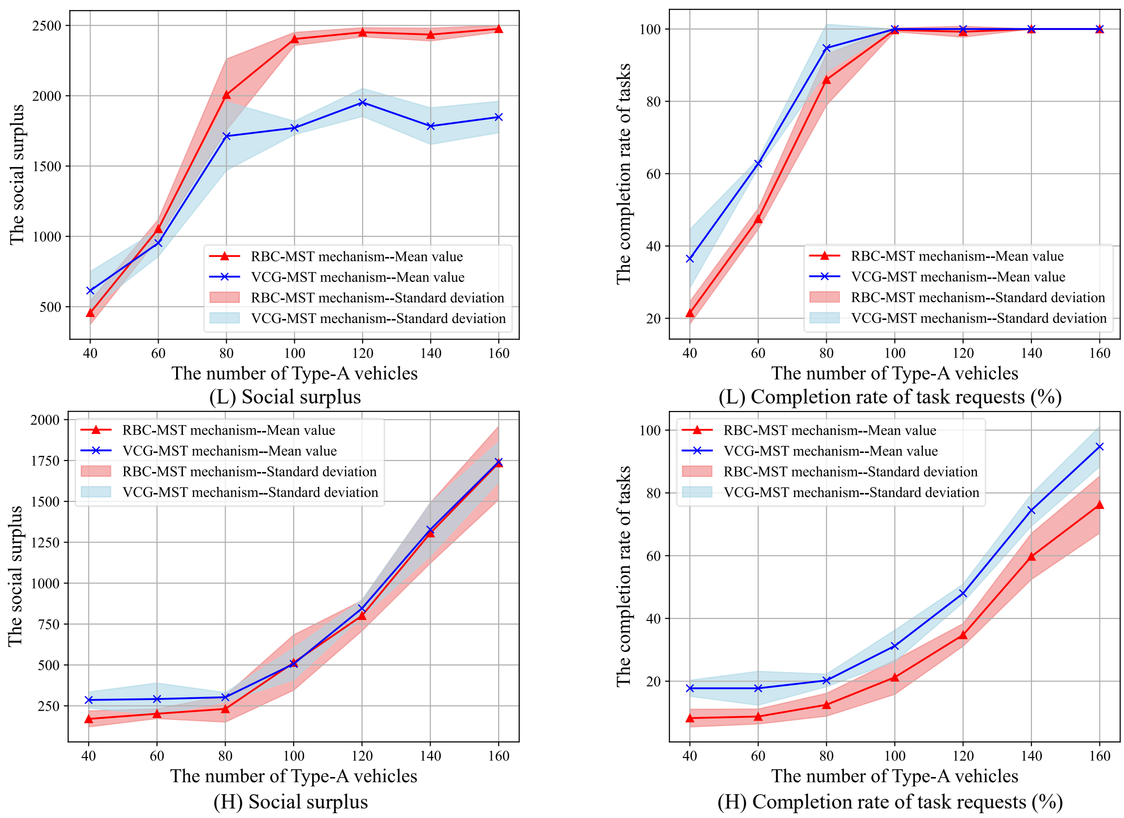

Figure 9: The impact of the various number of Type-A vehicles on MST assignment in (L) low travel demand scenario and (H) high travel demand scenario

5.4 Earning of the Type-A and Type-B drivers

Given the potential for generating high social surplus in scenarios with low travel demand, we may first investigate the earning of the drivers operating in the taxi-based mobile sensing business under these conditions. For this examination, we set the initial budget and fleet size to 2,000 and 140, respectively.

We might also wonder how to incentivize drivers to accept MSTs. As outlined in Table 2, the bid value per unit distance for vehicles ranges from 2 to 7. The lower bound corresponds to the unit income of Type-A drivers, while the upper bound is slightly smaller than the unit cost of dedicated vehicles. We can further subdivide this range into smaller increments, such as [2,4], [3,5], [4,6], and [5,7]. Conducting 5 repeated experiments for each range of bounds, we summarize the trip matching and MST assignment indices in Table 3. With increasing bid bounds, the average earning for Type-B drivers rises, though at the expense of social surplus and completion rate.

Table 3: The impact of performing sensing tasks under the low trip demand scenario

BD	Ω	N_{AB}	N_B	Trip matching		Task assignment		AP-A	AP-B
				AWT (s)	ATR (%)	ACR (%)	ASS		
$U[2,4]$	2000	140	20	59.30	98.1	100	2454.14	92.64	143.79
			25	61.41	98.1	100	2500.20	93.62	127.21
			30	61.78	98.1	100	2548.14	95.26	114.00
			35	63.30	98.1	100	2604.86	96.32	106.53
			40	62.56	98.2	100	2602.37	98.04	101.09
$U[3,5]$	2000	140	20	60.73	98.1	99.2	2309.17	92.79	147.10
			25	59.77	98.1	99.8	2352.15	94.00	130.38
			30	61.82	98.1	100	2419.38	94.79	119.97
			35	62.25	98.1	100	2455.92	95.65	112.68
			40	62.58	98.2	100	2474.72	98.79	102.39
$U[4,6]$	2000	140	20	60.15	98.1	94.5	1993.21	92.24	150.64
			25	61.04	98.1	98.2	2250.85	92.99	135.81
			30	61.56	98.1	97.0	2168.99	95.48	119.31
			35	62.09	98.1	99.8	2344.58	95.62	115.64
			40	64.02	98.1	99.8	2383.82	98.57	104.61
$U[5,7]$	2000	140	20	58.62	98.1	91.5	1882.55	91.83	152.62
			25	60.15	98.1	94.8	2031.39	93.64	132.74
			30	60.81	98.1	96.0	2116.25	95.72	118.84
			35	63.30	98.1	97.0	2202.87	97.22	110.41
			40	62.76	98.1	98.2	2227.72	97.58	108.19

Notes:
1. BD: the bounds of bids, N_{AB}: the total number of vehicles, N_B: the number of Type-B vehicles.
2. AWT: average waiting time, ATR: average trip matching rate, ACR: average completion rate, ASS: average social surplus.
3. AP-A: average earning of Type-A drivers, AP-B: average earning of Type-B drivers.

Figure 10 depicts the average earnings of Type-A and Type-B drivers across these experiments. When the count of Type-B vehicles is 30 or fewer, and the bid prices fall within the interval $[2, 4]$, Type-B drivers stand to earn significantly more than their Type-A counterparts by undertaking sensing tasks. Furthermore, the increment in the number of Type-B drivers doesn't markedly impact the earnings of Type-A drivers.

We conducted similar experiments in the high-demand scenario, and the key indices of trip matching and MST assignment are presented in Table 4. We observe that when the parameters are varied, the earnings trend for Type-A drivers is similar to that in the low-demand scenario. However, in scenarios where the number of Type-B vehicles is low, particularly in quantities equal to 20, The earning of Type-B drivers may not differ significantly from that of Type-A drivers, as depicted in Figure 11. This outcome is reasonable because, as shown in Table 4, when the number of Type-B vehicles is 20, the completion rate of sensing tasks is relatively low (approximately 30%), causing the earning of Type-B vehicles to largely derive from trip requests. Another interesting observation is that the average earning of Type-B drivers can

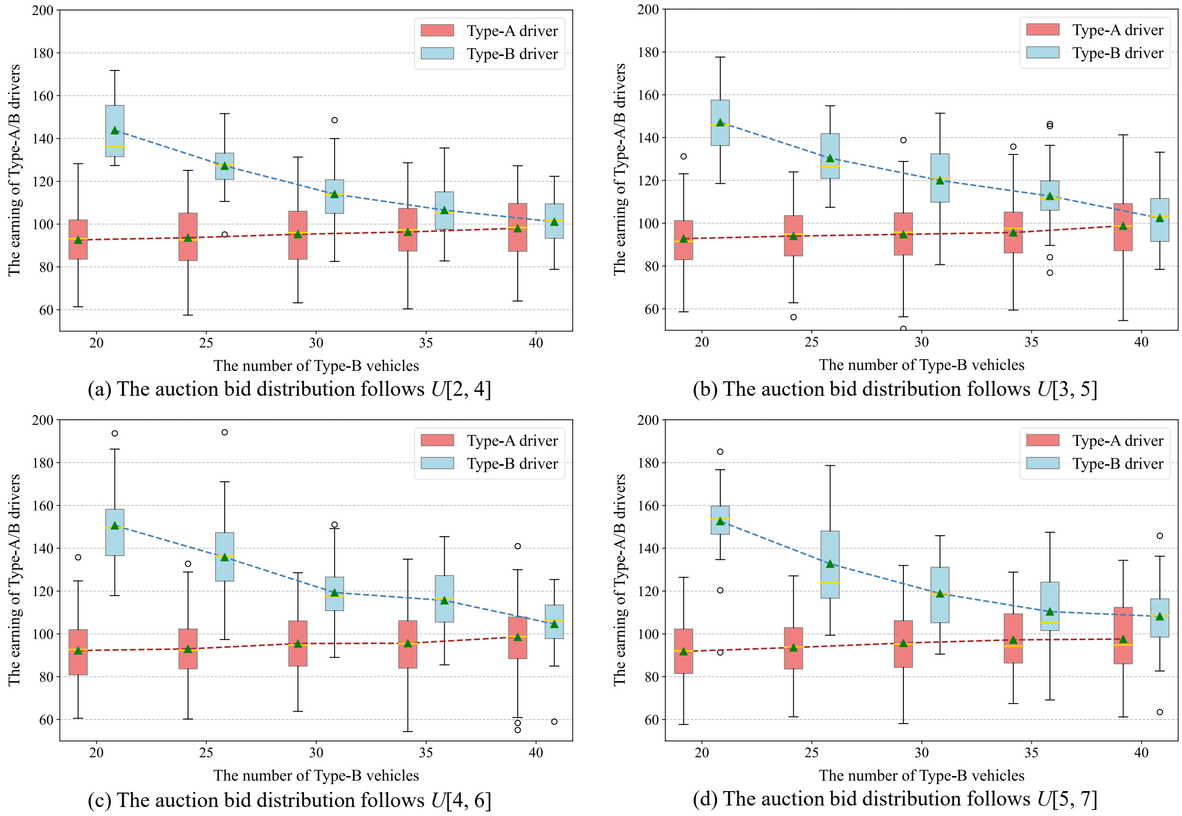

(a) The auction bid distribution follows $U[2, 4]$

(b) The auction bid distribution follows $U[3, 5]$

(c) The auction bid distribution follows $U[4, 6]$

(d) The auction bid distribution follows $U[5, 7]$

Figure 10: The average earning trend of Type-A drivers and Type-B drivers under the low trip demand scenario (constant initial budget and fixed fleet size)

slightly increase with the rise in the number of Type-B drivers. This could be because, as shown in Table 4, an increase in the number of Type-B vehicles leads to a higher completion rate of sensing tasks. Given that sensing tasks provide higher earnings compared to trip requests, completing a sufficient number of sensing tasks enables Type-B drivers to achieve greater earning. Moreover, the abundant availability of trip requests in the market ensures that Type-B drivers do not lose too many passenger service opportunities while fulfilling sensing tasks. Consequently, Type-B drivers can benefit from both trip requests and sensing tasks, thereby enabling them to achieve higher earnings compared to Type-A drivers.

6 Discussions and Conclusion

This study presents an operational strategy for mobile crowd-sensing using ride-hailing taxis. The strategy tailors task assignment rules for the two vehicle types in the ride-hailing system, prioritizing rider service levels. We address the order assignment problem by matching riders to Type-A and Type-B drivers, employing an auction-based mechanism to assign MSTs to ‘redundant’ Type-B drivers who have been idle for a significant duration. To ensure the data user’s benefit and incentivize ride-hailing platforms to engage in mobile sensing, we enhance the VCG mechanism by introducing a budget balance rule for winner selection. Additionally, we devise a novel payment rule to maintain platform budget balance. The RBC-MST mechanism, satisfying IC, IR, and BB properties, is developed as favorable for all ride-hailing system stakeholders. Various scenarios are tested to evaluate the integrated operational strategy and the RBC-MST mechanism. Results indicate that the proposed strategy achieves substantial social surplus while maintaining a satisfactory completion rate.

Another noteworthy observation is the benefit the RBC-MST mechanism provides to Type-B drivers who are inclined to undertake sensing tasks in most scenarios. But in the high trip

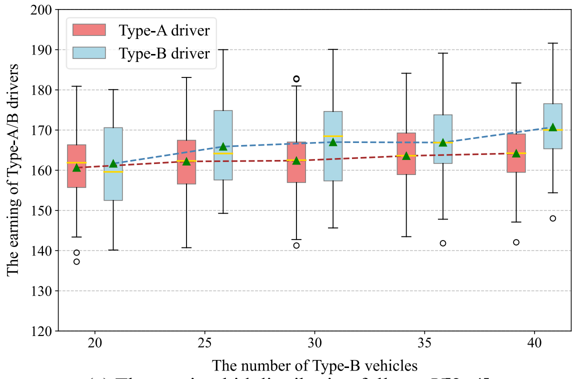

(a) The auction bid distribution follows $U[2, 4]$

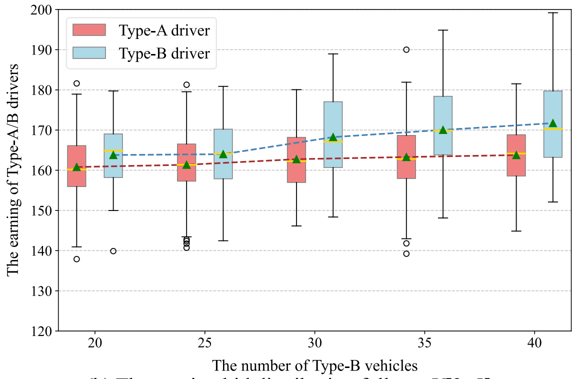

(b) The auction bid distribution follows $U[3, 5]$

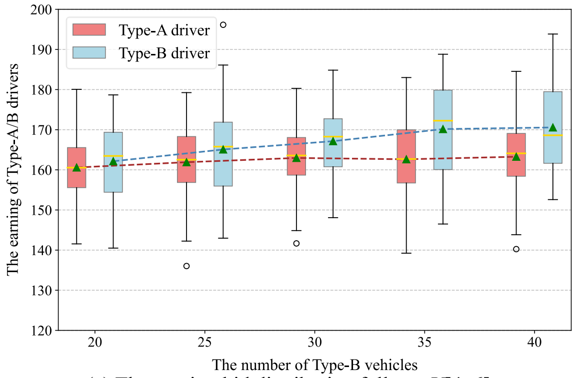

(c) The auction bid distribution follows $U[4, 6]$

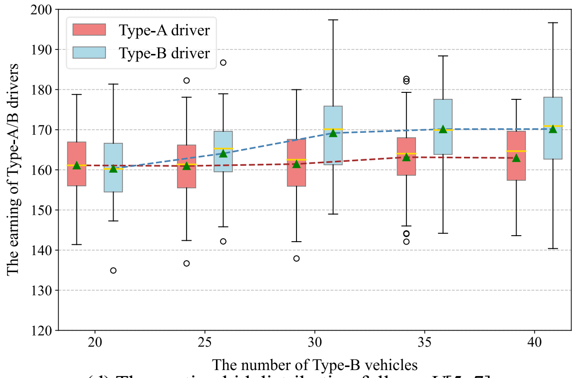

(d) The auction bid distribution follows $U[5, 7]$

Figure 11: The average earning trend of Type-A drivers and Type-B drivers under the high trip demand scenario (constant initial budget and fixed fleet size)

Table 4: The impact of performing sensing tasks under the high trip demand scenario

BD	Ω	N_{AB}	N_B	Trip matching		Task assignment		AP-A	AP-B
				AWT (s)	ATR (%)	ACR (%)	ASS		
$U[2,4]$	2000	140	20	103.39	96.0	33.25	675.73	160.64	161.67
			25	106.02	95.9	50.5	1173.24	162.19	165.89
			30	105.56	95.6	60	1355.34	162.39	167.01
			35	107.25	95.8	61.75	1488.73	163.58	166.90
			40	109.36	95.5	78.75	1885.15	164.20	170.72
$U[3,5]$	2000	140	20	103.86	96.3	31.75	563.01	160.80	163.79
			25	104.99	96.3	36.75	766.73	161.37	164.00
			30	105.39	96.1	51.25	999.34	162.75	168.25
			35	106.91	95.7	64.75	1365.66	163.29	170.04
			40	108.02	95.2	78.5	1803.68	163.78	171.73
$U[4,6]$	2000	140	20	102.99	96.1	28.5	564.13	160.58	162.14
			25	105.14	96.3	37.5	699.55	161.90	165.08
			30	108.55	96.1	49.5	973.06	162.96	167.14
			35	105.35	95.7	57.5	1147.68	162.63	170.16
			40	107.91	95.5	64.75	1222.36	163.27	170.56
$U[5,7]$	2000	140	20	103.07	96.4	25.5	464.07	161.12	160.32
			25	103.09	96.3	30.75	576.46	160.96	164.08
			30	105.22	96.0	42	742.93	161.45	169.17
			35	105.89	95.8	56.25	1085.71	163.15	170.13
			40	106.66	95.8	59	1149.74	162.97	170.17

Notes:
1. BD: distribution of bidding, N_{AB}: the total number of vehicles, N_B: the number of Type-B vehicles.
2. AWT: average waiting time, ATR: average trip matching rate, ACR: average completion rate, ASS: average social surplus.
3. AP-A: average earning of Type-A drivers, AP-B: average earning of Type-B drivers.

demand scenario, Type-B drivers may only marginally increase their average earnings from completing MSTs compared to serving riders. Additionally, they miss out on the opportunity to serve more riders in busy travel hubs. This issue could be addressed by introducing more Type-B vehicles into the ride-hailing system.

Although the proposed operation strategy and MST assignment mechanism effectively achieve our research objectives, there's room to tailor the methodology for more realistic scenarios. One direct extension could involve allowing Type-B drivers to handle both a ride-hailing request and one or multiple MSTs simultaneously. With appropriate route planning, a Type-B driver could efficiently complete MSTs during a detour while transporting a rider to their destination. This arrangement could potentially increase Type-B drivers' average earning and enhance their willingness to undertake MSTs. Fortunately, implementing this concept is not difficult by introducing a tri-partite shareable network of drivers, MSTs, and riders, as described in prior research (Alonso-Mora et al., 2017; Ge et al., 2021). Ideal drivers can be selected by solving a similar matching problem as the one presented in Section 4 on this shareable network.

Another issue worthy of investigation is budget allocation across plan cycles. While this paper discusses two rules–the *one-shot* rule and the *proportionality* rule–both are greedy and may not ensure optimal budget allocation. Alternatively, the budget for each plan cycle could be optimized by *learning* multi-day mobility and service patterns of drivers.

References

Agatz, N., Erera, A. L., Savelsbergh, M. W., Wang, X. (2011). Dynamic ride-sharing: A simulation study in metro Atlanta. Transportation Research Part B: Methodological, 45(9), 1450-1464.

Alnaggar, A., Gzara, F., Bookbinder, J. H. (2021). Crowdsourced delivery: A review of platforms and academic literature. Omega, 98, 102139.

Alonso-Mora, J., Samaranayake, S., Wallar, A., Frazzoli, E., Rus, D. (2017). On-demand high-capacity ride-sharing via dynamic trip-vehicle assignment. Proceedings of the National Academy of Sciences, 114(3), 462-467.

Archetti, C., Savelsbergh, M., Speranza, M. G. (2016). The vehicle routing problem with occasional drivers. European Journal of Operational Research, 254(2), 472-480.

Archetti, C., Guerriero, F., Macrina, G. (2021). The online vehicle routing problem with occasional drivers. Computers & Operations Research, 127, 105144.

Asprone, D., Di Martino, S., Festa, P., Starace, L. L. L. (2021). Vehicular crowd-sensing: a parametric routing algorithm to increase spatio-temporal road network coverage. International Journal of Geographical Information Science, 35(9), 1876-1904.

Bao, Y., Zang, G., Yang, H., Gao, Z., Long, J. (2023). Mathematical modeling of the platform assignment problem in a ride-sourcing market with a third-party integrator. Transportation Research Part B: Methodological, 178, 102833.

Bian, Z., Liu, X., Bai, Y. (2020). Mechanism design for on-demand first-mile ridesharing. Transportation research part B: methodological, 138, 77-117.

Chen, C., Pan, S., Wang, Z., Zhong, R. Y. (2017). Using taxis to collect citywide E-commerce reverse flows: a crowdsourcing solution. International Journal of Production Research, 55(7), 1833-1844.

Chen, X., Xu, S., Han, J., Fu, H., Pi, X., Joe-Wong, C., ... Zhang, P. (2020). Pas: Prediction-based actuation system for city-scale ridesharing vehicular mobile crowdsensing. IEEE Internet of Things Journal, 7(5), 3719-3734.

Cheng, M., Inci, E., Xu, S. X., Zhai, Y. (2023). A novel mechanism for private parking space sharing: The VickreyClarkeGroves auction with scale control. Transportation Research Part C: Emerging Technologies, 150, 104106.

Eriksson, J., Girod, L., Hull, B., Newton, R., Madden, S., Balakrishnan, H. (2008, June). The pothole patrol: using a mobile sensor network for road surface monitoring. In Proceedings of the 6th international conference on Mobile systems, applications, and services (pp. 29-39).

Fan, G., Jin, H., Liu, Q., Qin, W., Gan, X., Long, H., ... Wang, X. (2019). Joint scheduling and incentive mechanism for spatio-temporal vehicular crowd sensing. IEEE Transactions on Mobile Computing, 20(4), 1449-1464.

Ge, Q., Han, K., Liu, X. (2021). Matching and routing for shared autonomous vehicles in congestible network. Transportation research part E: logistics and transportation review, 156, 102513.

Guo, S., Qian, X., Dasgupta, S., Rahman, M., Jones, S. (2022). Sensing and monitoring of urban roadway traffic state with large-scale ride-sourcing vehicles. The Rise of Smart Cities, 551-582.

Hammami, F., Rekik, M., Coelho, L. C. (2021). Exact and hybrid heuristic methods to solve the combinatorial bid construction problem with stochastic prices in truckload transportation services procurement auctions. Transportation Research Part B: Methodological, 149, 204-229.

Hanzhi, 2024. Driver surplus and intense competition among platforms: outlook of the ride-hailing market in 2024 (in Chinese). Retrieved 2024-1-18, from https://www.yicai.com/news/101960804.html.

Han, K., Ji, W., Nie, Y. M., Li, Z., Liu, S. (2024). Exploring the sensing power of mixed vehicle fleets. Transportation Research Part B: Methodological, 190, 103066.

Hasenfratz, D., Saukh, O., Walser, C., Hueglin, C., Fierz, M., Arn, T., ..., Thiele, L. (2015). Deriving high-resolution urban air pollution maps using mobile sensor nodes. Pervasive and Mobile Computing, 16, 268-285.

Jezdovi, I., Popovi, S., Radenkovi, M., Labus, A., Bogdanovi, Z. (2021). A crowdsensing platform for real-time monitoring and analysis of noise pollution in smart cities. Sustainable Computing: Informatics and Systems, 31, 100588.

Ji, W., Han, K., Liu, T. (2023). A survey of urban drive-by sensing: An optimization perspective. Sustainable Cities and Society, 104874.

Ji, W., Liu, S., Han, K., Li, Y., Liu, T. (2024). The Share-a-Ride Problem with mixed ride-hailing and logistic vehicles. Transportation Research Part E: Logistics and Transportation Review, 192, 103758.

Karamanis, R., Anastasiadis, E., Angeloudis, P., Stettler, M. (2020). Assignment and pricing of shared rides in ride-sourcing using combinatorial double auctions. IEEE Transactions on Intelligent Transportation Systems, 22(9), 5648-5659.

Kong, X. T., Zhu, M., Liu, Y., Qin, K., Huang, G. Q. (2023). An advanced order batching approach for automated sequential auctions with forecasting and postponement. International Journal of Production Research, 61(12), 4180-4195.

Krishna V. (2009). Auction Theory, Second ed. (Academic Press, Burlington, MA).

Li, B., Krushinsky, D., Reijers, H. A., Van Woensel, T. (2014). The share-a-ride problem: People and parcels sharing taxis. European Journal of Operational Research, 238(1), 31-40.

Li, R., Nie, Y., Liu, X. (2020). Pricing carpool rides based on schedule displacement. Transportation Science, 54(4), 1134-1152.

Li, Y., Li, Y., Peng, Y., Fu, X., Xu, J., Xu, M. (2022). Auction-based crowdsourced first and last mile logistics. IEEE Transactions on Mobile Computing, 23(1), 180-193.

Li, R., Liu, Y., Liu, X., Nie, Y. M. (2024). Allocation problem in cross-platform ride-hail integration. Transportation Research Part B: Methodological, 188, 103056.

Mancini, S., Gansterer, M. (2022). Bundle generation for last-mile delivery with occasional drivers. Omega, 108, 102582.

Masutani, O. (2015, March). A sensing coverage analysis of a route control method for vehicular crowd sensing. In 2015 IEEE International Conference on Pervasive Computing and Communication Workshops (PerCom Workshops) (pp. 396-401). IEEE.

Mochon, P., Mochon, A., Saez, Y. (2022). Combinatorial versus sequential auctions to allocate PPP highway projects. Transport Policy, 117, 23-39.

NYC Taxi and Limousine Commission, 2022. TLC trip record data. Retrieved 2023-6-28, from https://www.nyc.gov/site/tlc/about/tlc-triprecord-data.page.

O'Keeffe, K. P., Anjomshoaa, A., Strogatz, S. H., Santi, P., Ratti, C. (2019). Quantifying the sensing power of vehicle fleets. Proceedings of the National Academy of Sciences, 116(26), 12752-12757.

Qi, W., Li, L., Liu, S., Shen, Z. J. M. (2018). Shared mobility for last-mile delivery: Design, operational prescriptions, and environmental impact. Manufacturing & Service Operations Management, 20(4), 737-751.

Statista, 2023. Ride-hailing - united states. Retrieved 2024-1-18,from https://www.statista.com/outlook/mmo/shared-mobility/shared-rides/ridehailing/united-states

Tafreshian, A., Masoud, N. (2022). A truthful subsidy scheme for a peer-to-peer ridesharing market with incomplete information. Transportation Research Part B: Methodological, 162, 130-161.

Uber-UK, 2023. Uber aims to be wider travel app as it turns first profit. Retrieved 2024-1-8, from https://www.bbc.com/news/business-66375733.

Wang, H., Yang, H. (2019). Ridesourcing systems: A framework and review. Transportation Research Part B: Methodological, 129, 122-155.

Wang, Y., Wu, C., Zhu, T. (2019). Mobile hailing technology and taxi driving behaviors. Marketing Science, 38(5), 734-755.

Wu, Y., Wang, Y., Wang, L., Song, G., Gao, J., Yu, L. (2020). Application of a taxi-based mobile atmospheric monitoring system in Cangzhou, China. Transportation research part D: transport and environment, 86, 102449.

Xu, S. X., Huang, G. Q., Cheng, M. (2017). Truthful, budget-balanced bundle double auctions for carrier collaboration. Transportation science, 51(4), 1365-1386.

Xu, S., Chen, X., Pi, X., Joe-Wong, C., Zhang, P., Noh, H. Y. (2019). ilocus: Incentivizing vehicle mobility to optimize sensing distribution in crowd sensing. IEEE Transactions on Mobile Computing, 19(8), 1831-1847.

Yan, P., Lee, C. Y., Chu, C., Chen, C., Luo, Z. (2021). Matching and pricing in ride-sharing: Optimality, stability, and financial sustainability. Omega, 102, 102351.

You, J., Jiang, H., Chen, Z., Ming, X., Sun, P. Z. (2023). Order allocation strategy for online car-hailing platform in the context of multi-party interests. Advanced Engineering Informatics, 57, 102110.

Zhang, Y., Li, B., Krishnan, R. (2020). Learning individual behavior using sensor data: The case of global positioning system traces and taxi drivers. Information Systems Research, 31(4), 1301-1321.

Zhou, Y., Yang, H., Ke, J., Wang, H., Li, X. (2022). Competition and third-party platform-integration in ride-sourcing markets. Transportation Research Part B: Methodological, 159, 76-103.

Zou, B., Kafle, N. (2023). Designing mechanisms for crowdsourced urban parcel delivery. Transportation Letters, 15(8), 992-1010.